

UCSF

UC San Francisco Electronic Theses and Dissertations

Title

GENETIC AND EVOLUTIONARY APPROACHES TO TRANSIENT RECEPTOR POTENTIAL CHANNEL STRUCTURE AND FUNCTION

Permalink

<https://escholarship.org/uc/item/70f4p5dj>

Author

Myers, Benjamin

Publication Date

2008

Peer reviewed|Thesis/dissertation

Genetic and Evolutionary Approaches to
Transient Receptor Potential Channel Structure and Function

by

Benjamin R. Myers

DISSERTATION

Submitted in partial satisfaction of the requirements for the degree of

DOCTOR OF PHILOSOPHY

in

Cell Biology

in the

GRADUATE DIVISION

of the

UNIVERSITY OF CALIFORNIA, SAN FRANCISCO

ACKNOWLEDGMENTS

Graduate school at UCSF has been an incredibly worthwhile and rewarding experience, both intellectually and personally. None of the research presented in my thesis would have been possible without the support of many friends, coworkers, and family members throughout this phase of my scientific journey.

First, I would like to thank my mentor, David Julius, for his advice and support over the last six years. David is creative, fearless, and combines an enthusiasm for research with a remarkably broad perspective on biology, all of which I hope to emulate in the future as an independent scientist. David taught me a great deal about how to formulate and tackle a research question and guided me patiently through my (oftentimes slow) process of scientific maturation. I would also like to thank the other members of my thesis committee, Dan Minor, Roger Nicoll, and Mark von Zastrow, who always provided helpful advice during our regular meetings. I am particularly indebted to Dan for providing technical and intellectual advice at each phase of my research.

I learned a great deal from many talented scientists working in David's lab. Huai-hu Chuang was both an instructor in the technique of patch clamp electrophysiology, as well as a mentor whose advice helped me navigate around many of the scientific obstacles I encountered during my projects. Huai-hu was always extremely patient and generous with his time whenever I had questions or concerns, and my research benefited enormously as a result of his creative and insightful suggestions. I would also like to thank Chris Bohlen and Yari Sigal, two graduate students who collaborated with me on several of the experiments described here, as well as Anna Ermund, who provided valuable technical assistance early on in graduate school. Pam Tsuruda and Gunther Hollopeter taught me a great deal about molecular biology and provided a

continual source of lab antics. Diana Bautista, Alex Chesler, and Avi Priel gave valuable feedback on my project and helpful comments on initial manuscripts. Jeannie Poblete continues to work quietly but diligently to ensure that the members of Julius lab are well equipped for their experiments.

UCSF has been a fantastic environment in which to work as a graduate student. I would like to thank Jonathan Weissman, Hiten Madhani, Yuriy Kirichok, and members of their labs, all of who went out of their way to answer my questions and provide reagents. I would also like to thank my classmates for many insightful and entertaining discussions, as well as the Tetrad staff for helping our graduate program run smoothly.

I owe a great deal to my family, who has provided unconditional love and supported all of my education and career choices, and I very much appreciate their confidence and encouragement throughout graduate school. Outside of lab, I feel very fortunate to have a wonderful group of friends who always ensured that I did not take life too seriously. And finally, the love I have shared with Ta-Chen Wang during the last five years has enriched my life immeasurably.

Chapter 2, “A Yeast Genetic Screen Reveals a Critical Role for the Pore Helix Domain in TRP Channel Gating”, was previously published (*Neuron* 58, 362–373, May 8, 2008) and has been reprinted with permission from Elsevier, Ltd.

**GENETIC AND EVOLUTIONARY APPROACHES TO TRANSIENT RECEPTOR
POTENTIAL CHANNEL STRUCTURE AND FUNCTION**

by Benjamin Myers

ABSTRACT

Transient Receptor Potential (TRP) cation channels function as cellular sensors in uni- and multicellular eukaryotes. Despite intensive study, the mechanisms of TRP channel activation by chemical or physical stimuli remain poorly understood. Here we present strategies to unravel these biophysical mechanisms based on genetic and evolutionary approaches. First, to identify amino acid residues crucial for TRP channel gating, we developed an unbiased, high-throughput genetic screen in yeast that uncovered rare, constitutively active mutants of the capsaicin receptor, TRPV1. We show that mutations within the pore helix domain dramatically increase basal channel activity and responsiveness to chemical and thermal stimuli. Mutation of corresponding residues within two related TRPV channels leads to comparable effects on their activation properties. Our data suggest that conformational changes in the outer pore region are critical for determining the balance between open and closed states, providing evidence for a general role for this domain in TRP channel activation. We also report the cloning and characterization of an ortholog of a cold and menthol receptor, TRPM8, from the cold-blooded African clawed frog *Xenopus laevis*. This TRPM8 ortholog responds to menthol but displays a striking shift in its temperature-response profile toward lower temperatures compared to the rat and chicken receptors, with a positive correlation between TRPM8 response threshold and species core body temperature. Our results suggest that species-specific differences in thermosensitivity can be attributed at least in part to intrinsic biophysical properties of temperature-gated channels in peripheral sensory neurons.

TABLE OF CONTENTS

Chapter 1. Introduction	1
Chapter 2. A Yeast Genetic Screen Reveals a Critical Role for the Pore Helix Domain in TRP Channel Gating	11
Chapter 3. A Cold-activated TRP Channel Ortholog from <i>Xenopus laevis</i> Displays Alterations in Responsiveness to Thermal Stimuli	58
Chapter 4. Bibliography	89

LIST OF TABLES AND FIGURES

Figure 1.	35
Figure 2.	37
Figure 3.	39
Figure 4.	41
Figure 5.	43
Figure 6.	45
Figure 7.	47
Figure 8.	49
Figure 9.	51
Figure 10.	53
Figure 11.	74
Figure 12.	76
Figure 13.	78
Figure 14.	80
Figure 15.	82
Figure 16.	84
Figure 17.	86
Table 1.	55
Table 2.	56
Table 3.	88

CHAPTER 1.

Introduction

Mammals Sense their Environments

The ability of an organism to sense and respond to cues in its environment is one of the most fundamental processes in biology. In keeping with the importance of sensory input for survival and well-being, multicellular organisms such as mammals have evolved sophisticated physiological systems dedicated exclusively to sensing the features of their environments. The visual, olfactory, auditory, and gustatory branches of the peripheral nervous system are responsible for detection of sight, smell, sound, and taste, respectively. The senses of touch, temperature, pain, and proprioception belong to the mammalian somatosensory system (Kandel et al., 2000).

Somatosensory neurons perform the task of nociception, the process of sensing and interpreting noxious or pain-producing environmental stimuli. A key to the molecular basis of nociception is the specific expression by somatosensory neurons of a unique complement of excitatory receptors for noxious chemical and physical agents, spanning a wide range of pharmacological irritants, temperatures, and mechanical stimuli. In mammals, the cell bodies of somatosensory neurons reside in the trigeminal and dorsal root ganglia, and together these neurons innervate the head, neck, trunk, arms, and legs (Fields, 1987; Kandel et al., 2000). Upon exposure to a noxious agent, ionotropic receptors expressed on the somatosensory nerve terminal are activated, and the subsequent depolarizing influx of cations triggers an action potential that is relayed back to the neuron's cell body. The information encoded in this action potential is ultimately transmitted to the central nervous system as a pain signal. The stimulus-evoked excitation of somatosensory receptors is therefore the first in a multi-step pathway indicating the presence of a harmful or noxious agent in our environment (Fields, 1987; Kandel et al., 2000).

Sensory Neuronal TRP Channels are Receptors for Noxious Chemical and Physical Stimuli

In the past decade, a tremendous amount of progress has been made in identifying and characterizing the excitatory receptors that allow somatosensory neurons to respond to noxious thermal stimuli. An important step in this process turned out to be the recognition that chemical compounds mimicking the psychophysical sensations of hot and cold temperatures could be used as pharmacological probes in forward genetic strategies to clone excitatory thermosensitive receptors (Julius, 2005). Thus, capsaicin, the spicy ingredient in “hot” chili peppers, led to the identification of transient receptor potential V1 (TRPV1), a cation channel that also responds to noxious heat ($> 43^{\circ}\text{C}$) and pro-inflammatory agents such as extracellular protons (Caterina et al., 1997; Tominaga et al., 1998). Upon exposure to any of these stimuli, TRPV1 is activated, leading to cation influx and action potential generation in sensory neurons (Julius and Basbaum, 2001). Similarly, menthol, a cooling compound originating from the mint plant, targets TRPM8, a sensor of moderate cold ($<26^{\circ}\text{C}$) (McKemy et al., 2002; Peier et al., 2002a). Finally, allyl isothiocyanate (mustard oil), a pungent ingredient in wasabi and mustard, activates TRPA1, an irritant receptor (Jordt et al., 2004). Mice deficient in each of these sensory TRP channels display profound defects in responses to cognate chemical and/or thermal stimuli at both cellular and behavioral levels (Bautista et al., 2006; Bautista et al., 2007; Caterina et al., 2000; Colburn et al., 2007; Davis et al., 2000; Dhaka et al., 2007; Kwan et al., 2006), indicating that these TRP channels play a physiologically relevant function as environmental sensors in somatosensory neurons.

One of the most fascinating features of sensory TRP channels is their polymodal activation. While most other families of sensory receptors have evolved to recognize a

single type of cognate ligand, each of the sensory TRP channels described above seems able to sense an extremely wide set of chemical and physical agonists simultaneously (Jordt et al., 2003; Julius, 2005). Moreover, the responses of a given TRP channel to one agonist can be influenced by the presence of another agonist. For example, TRPV1 responses to capsaicin are enhanced by a low level of extracellular protons, by a moderate rise in ambient temperature, or by activation of a phospholipase C (PLC)-coupled signaling pathway (which releases TRPV1 from a tonic PIP₂-mediated inhibition) (Chuang et al., 2001; Tominaga et al., 1998). Such findings illustrate that TRP channels not only have the capacity to sense a broad range of stimuli, but also integrate signals from multiple diverse chemical and physical agonists into a single response. This polymodal processing enables TRP channels to rapidly alter their properties, enabling optimal responsiveness under a range of physiological conditions. Such plasticity is perhaps clearest for TRPV1 under conditions of tissue injury, where the presence of extracellular protons or proinflammatory mediators that activate PLC-coupled signaling pathways can modulate TRPV1 responses to capsaicin or noxious heat, leading to enhanced channel sensitivity appropriate within the setting of inflammation (Chuang et al., 2001; Julius and Basbaum, 2001; Tominaga et al., 1998).

TRP Channels: A Large and Diverse Superfamily of Molecular Sensors

As their names imply, the three sensory TRP channels described above are part of the same superfamily of ion channels, with members in nearly all eukaryotic species from yeast to man (Clapham, 2003; Dhaka et al., 2006; Venkatachalam and Montell, 2007). The founding member of this superfamily is the canonical *Drosophila* TRP channel expressed in its photoreceptor cell and required for sustained depolarizing responses to light. There are 27 known TRP channels in humans, 28 in mice, 13 in flies, and 17 in worms (Venkatachalam and Montell, 2007). Animal TRP channels can be loosely

grouped on the basis of sequence similarity into seven subfamilies: TRPV, TRPC, TRPM, TRPA, TRPP, TRPML, and TRPN. However, because TRP channels are highly divergent at the level of primary amino sequence, sometimes exhibiting less than 20% amino acid identity even within the same subfamily¹, sequence-based classifications must be interpreted with caution. The precise physiological function of many TRP channels is still a matter of debate. Although only a subset of TRP channels are thought to participate directly in somatosensation, TRP channels may play a more general function as sensors of the cellular milieu (Clapham, 2003; Dhaka et al., 2006; Venkatachalam and Montell, 2007).

Comparison of TRP Channels Across Evolution Suggest Partial Conservation of Function

Many TRP channels are expressed in orthologous form throughout evolution¹, and while the activation properties and physiological function of the main sensory neuronal TRP channels (TRPV1, TRPM8, TRPA1) have been probed most extensively in rodents, these channels are clearly present in the genomes of many other species as well. TRPA1 is likely the most evolutionarily ancient of the sensory TRP's, as it can be traced to *Drosophila* and *C. elegans* (Venkatachalam and Montell, 2007). TRPV1 sequences can be identified in several fish genomes including zebrafish. TRPM8 is the newest of these channels in evolutionary terms, as it can be found in an amphibian genome but appears to be absent from pre-tetrapod evolution (Saito and Shingai, 2006).

In some respects, perhaps this evolutionary conservation of sequences for sensory TRP

¹ In some cases, TRP channels display substantially higher sequence identity to orthologs from distantly related species than to other family members from the same species. For example, rat TRPM8 displays only 40% sequence identity with rat TRPM2 (its closest relative within the TRPM subfamily), but displays more than 70% sequence identity with *Xenopus laevis* TRPM8 (see chapter 3).

channels is not surprising, since many of the major ionotropic and metabotropic receptors studied in mammals, including voltage-gated channels and neurotransmitter receptors, are also highly conserved. The evolutionary conservation of TRP channel sequences implies that, at some level, the underlying molecular logic of signal reception in somatosensory neurons is also likely to be similar between species. Nevertheless, the role of TRP channels as environmental sensors implies a strong connection between the physiological properties of these receptors and a species' ecological niche. Given the wide variation in environments inhabitable by different species, it is reasonable to expect that, if TRP channels indeed contribute to somatosensory biology in a wide range of species, then within a given species TRP channel properties may be under strong evolutionary pressures to conform to the most appropriate set of environmental conditions.

To what degrees do the properties of sensory TRP channels vary across evolution? The physiology of sensory TRP channels outside of rodents and humans, particularly in animals other than mammals, has not been extensively investigated to date. An ortholog of TRPV1 was cloned from chickens, which are known to be insensitive at the behavioral level to the effects of capsaicin. This property was reflected in the failure of chicken TRPV1 to undergo activation by capsaicin, although it retained sensitivity to protons and noxious heat (Jordt and Julius, 2002). Along similar lines, chicken TRPM8 proved insensitive to icilin, a synthetic super-cooling compound that may act to mimic an endogenous mammalian small molecule, but was sensitive to menthol and cold (Chuang et al., 2004). While mustard oil activation of *Drosophila* TRPA1 has not been reported, the two copies of zebrafish TRPA1 both displayed mustard oil sensitivity (Prober et al., 2008), arguing that this receptor modality is at least partially conserved throughout evolution. Thus, although some pharmacological properties of TRP channels are highly

conserved, others appear to be altered in the course of evolution depending on the needs of a particular organism's somatosensory system.

Towards a Structural and Function Basis for the Activation of TRP Channels

Despite their modest homology at the amino acid level, TRP channels are predicted to share a common topology. Most TRP channels are thought to assemble in the membrane as homomeric tetramers. Each channel subunit is predicted to possess six transmembrane domains (S1-S6), with a pore loop between S5 and S6, and intracellular N- and C-termini. This predicted topology places TRP channels within the same "6TM" superfamily as voltage-gated Na⁺, K⁺, and Ca²⁺ channels, whose structure, function, and physiology have been probed in great detail (Clapham, 2003; Dhaka et al., 2006; Venkatachalam and Montell, 2007). Indeed, there is a great wealth of information concerning the biophysical basis for activation of voltage-gated channels, although the precise mechanism of voltage activation is still a matter of debate (Tombola et al., 2006; Yellen, 1998). In addition, recent K⁺ channel crystal structures (Long et al., 2005a, b) not only yield a high-resolution view of the voltage gating process for these channels but also offer a glimpse of how TRP channel sequences might appear in three-dimensional form. However, a number of important differences between TRP and voltage-gated channels preclude the wholesale use of such models to understand TRP channel activation. First, TRP and voltage-gated channels are extremely distantly related in sequence. Second, TRP channels are only weakly gated by voltage, and they do not contain the cluster of positively charged arginine residues within their S4 helix that is the sequence hallmark of a voltage sensor domain. Finally, there is not yet any crystallographic data for a full-length TRP channel, making it difficult to directly determine which aspects of their three-dimensional conformation, if any, are similar to those of voltage-gated channels.

Several sequence elements within individual TRP channels have been identified as participating in agonist binding or channel gating. For TRPV1, capsaicin is thought to bind within the cytoplasmic linker between the second and third transmembrane helices (Jordt and Julius, 2002), while pH is thought to influence channel gating by influencing the protonation state of aspartate residues at or near the extracellular face of the channel (Jordt et al., 2000). PIP₂ has been suggested to tonically inhibit TRPV1 by binding to a C-terminal region rich in positive charges (Prescott and Julius, 2003), although it has been suggested that other regions of TRPV1 may be involved in mediating the apparently complex functional interactions of PIP₂ with this channel (Lishko et al., 2007; Lukacs et al., 2007; Ryu et al., 2007). Intriguingly, the same TM2-3 linker shown to mediate capsaicin effects on TRPV1 has been implicated in icilin binding for TRPM8, suggesting that this region may be conserved in multiple TRP channels as an agonist binding site (Chuang et al., 2004). Structural determinants of menthol activation within the transmembrane and C-terminal regions of TRPM8 have also been identified (Bandell et al., 2006). Gating of TRPA1 by mustard oil, which is inherently electrophilic, proceeds via an unusual mechanism involving covalent modification of cysteines within the channel's N-terminus (Bandell et al., 2006; Hinman et al., 2006; Macpherson et al., 2007). While it is unclear how such N-terminal TRPA1 residues might induce a conformational change that regulates channel opening, a recent structural and functional study of the TRPV1 N-terminus suggests that this cytoplasmic region of TRP channels might prove to be a critical part of their gating apparatus (Lishko et al., 2007; Myers and Julius, 2007). There is currently little information on the molecular basis for TRPV1 or TRPM8 activation by temperature, although one study suggests a critical role for the C-terminal channels tails in determining responsiveness to heat versus cold (Brauchi et al., 2006).

The identification of numerous structural elements mediating ligand binding raises two broad, outstanding questions concerning TRP channel structure and function. First, in many cases it is unclear how conformational changes induced by agonist binding to the channel are communicated allosterically to the pore region to regulate overall channel opening or closing. Second, few discrete sequence elements that regulate the gating of multiple TRP channels have been identified, making it difficult to assess whether gating of the diverse members of this large channel family share any common structural or mechanistic features.

Genetic and Evolutionary Approaches to TRP Channel Biology

Here, I attempt to use genetic and evolutionary approaches to answer two separate questions related to the function and physiology of TRP channels. In chapter 2, I focus on identifying and characterizing regions or residues within TRP channels that are critical for their gating by chemical and thermal stimuli. To begin to answer this question, I employ a forward genetic screening methodology to uncover, in an unbiased fashion, mutations within TRP channel sequences that lead to aberrant gating behavior. This screen led to the finding that the pore helix domain controls the gating of at least three different TRP channels. In chapter 3, I address the degree to which the thermal activation properties of sensory neuronal TRP channels are conserved throughout animal evolution by examining the properties of TRPV1 and TRPM8 orthologs cloned from *Xenopus laevis*, a cold-blooded aquatic frog whose habitat differs substantially from that of rats, mice, and humans. I find a dramatic shift in the thermal gating of *Xenopus laevis* TRPM8 compared to its mammalian or avian counterparts, such that the frog channel requires far colder temperatures to achieve substantial activation, supporting a model wherein the properties of TRP channels are altered throughout evolution to allow

for thermal sensory transduction within a temperature range most appropriate to an organism's ecological niche.

CHAPTER 2.

A Yeast Genetic Screen Reveals a Critical Role for the Pore Helix Domain in TRP Channel Gating

ABSTRACT

TRP cation channels function as cellular sensors in uni- and multicellular eukaryotes. Despite intensive study, the mechanisms of TRP channel activation by chemical or physical stimuli remain poorly understood. To identify amino acid residues crucial for TRP channel gating, we developed an unbiased, high-throughput genetic screen in yeast that uncovered rare, constitutively active mutants of the capsaicin receptor, TRPV1. We show that mutations within the pore helix domain dramatically increase basal channel activity and responsiveness to chemical and thermal stimuli. Mutation of corresponding residues within two related TRPV channels leads to comparable effects on their activation properties. Our data suggest that conformational changes in the outer pore region are critical for determining the balance between open and closed states, providing evidence for a general role for this domain in TRP channel activation.

INTRODUCTION

Members of the transient receptor potential (TRP) family of nonselective cation channels participate in a wide variety of physiological processes in organisms ranging from fungi to humans (Clapham, 2003; Dhaka et al., 2006; Venkatachalam and Montell, 2007). TRP channels respond to such diverse agonists as hypertonicity in yeast, light-evoked phospholipase C (PLC) activation in the *Drosophila* photoreceptor, and noxious chemical and thermal stimuli in the mammalian somatosensory system. Accordingly, spontaneous loss- and gain-of-function mutations in TRP channels underlie disease states resulting from decreased or increased cation influx, respectively (Nilius, 2007). TRP channels belong to the six-transmembrane-domain (6TM, S1-S6) cation channel superfamily that includes depolarization-activated K^+ , Na^+ , and Ca^{2+} channels, as well as cyclic-nucleotide-gated (CNG) and hyperpolarization-activated (HCN) channels. TRP channels fall into several subfamilies, including vanilloid (V), canonical (C), and melastatin (M)

groups, with most members suspected to form tetramers *in vivo*. Based on hydropathy predictions, each subunit contains intracellular N- and C-termini and a membrane-reentrant pore loop between S5 and S6. As a class, TRP channels bear resemblance at the level of transmembrane topology but show remarkably little primary sequence homology within and across subfamilies (Clapham, 2003).

TRP channels respond to an array of stimuli, including physical and chemical agonists (Clapham, 2003; Dhaka et al., 2006; Venkatachalam and Montell, 2007). For example, TRPV1, the founding member of the vanilloid subfamily, is the receptor for capsaicin (the pungent ingredient in “hot” chili peppers), but also responds to extracellular protons, bioactive lipids, and noxious heat (>43°C) (Caterina et al., 1997; Jordt et al., 2003; Siemens et al., 2006; Tominaga et al., 1998). Like many other members of the TRP channel family, TRPV1 can also be modulated by PLC-coupled signal transduction pathways (Chuang et al., 2001; Lukacs et al., 2007; Prescott and Julius, 2003). However, the molecular mechanisms underlying TRP channel activation, ranging from stimulus detection to the regulation of channel opening (gating), are poorly understood. This stands in contrast to other 6TM channels, most notably voltage-activated K⁺ channels, which have been probed in great detail using biophysical and crystallographic methods (Tombola et al., 2006; Yellen, 1998).

For voltage-gated channels, an important clue to their common activation mechanism came from visual inspection of linear protein sequences, which revealed a discrete domain (the positively charged S4 helix) as a likely universal candidate for translating changes in plasma membrane voltage into channel opening (Tombola et al., 2006; Yellen, 1998). In contrast, TRP channels are activated by a diversity of chemical and physical stimuli for which corresponding functional motifs are not readily apparent in the

channel polypeptide (Clapham, 2003), making it challenging to gain insight into the gating process. Furthermore, TRP and voltage-gated channels are not only functionally divergent, but also show sparingly little sequence similarity. Thus, the use of previously developed structural and mechanistic models to ascertain TRP channel function is rather limited. This leaves unanswered the important question of whether any unifying mechanistic principles underlie TRP channel gating.

While previous reports have delineated molecular determinants for agonist binding and activation in several TRP family members, including TRPV1 (Jordt and Julius, 2002; Jordt et al., 2000; Jung et al., 2002), few, if any, conserved structural elements controlling TRP channel gating have been reported. The difficulty in pinpointing critical gating domains stems, in part, from the challenge of conducting mutational analyses that efficiently sample a large sequence space. Conventional ion channel structure-function studies generally entail the construction and testing of channel mutants one at a time; such studies are low-throughput, precluding an unbiased examination in which multiple substitutions at each sequence position are evaluated for functional alterations. Some studies have exploited amino acid polymorphisms between functionally divergent TRP channel family members to narrow down blocks of sequence that contain determinants of agonist activation (via analysis of chimeric channels) (Chuang et al., 2004; Jordt and Julius, 2002), but this methodology is poorly suited to uncovering core structural elements which are expected to show high levels of conservation among TRP channels. Such limitations can be partially overcome by using robotic methods to sample large numbers of individual mutants via high-throughput functional assays (Bandell et al., 2006; Decaillet et al., 2003; Zhou et al., 2007). Alternatively, genetic strategies based on simple life-or-death readouts (Loukin et al., 1997; Minor et al., 1999; Ou et al., 1998)

could permit selection of functionally interesting channel mutants, but such a methodology has not been applied to mammalian TRP channels.

Here we describe the identification and characterization of a critical component of the TRP channel gating machinery via unbiased genetic screening of a randomly generated population of TRPV1 mutants. We conducted this high-throughput screen on mammalian TRPV1 heterologously expressed in the budding yeast *Saccharomyces cerevisiae*, whose superior genetics allows for the efficient isolation of constitutively active channel alleles. Our study reveals that gain-of-function substitutions in the pore helix of TRPV1 dramatically affect channel activation, establishing an important role for this domain in TRPV1 functionality. We extend these observations to two other members of the TRPV subfamily, suggesting that the pore helix is a key regulatory domain that plays a conserved role in the gating of at least a subset of excitatory TRP channels.

RESULTS

Functional Expression of the Capsaicin Receptor in Yeast

Persistent activation of native or recombinant vanilloid receptors leads to a dramatic decrease in mammalian cell viability due to overload with cations (Caterina et al., 1997; Jancso et al., 1977; Winter, 1987; Wood et al., 1988). We reasoned that if TRPV1 forms functional channels upon heterologous expression in yeast, then exposure to capsaicin should be fatal. Indeed, yeast transformed with TRPV1 grew robustly on standard solid medium, but failed to grow on medium containing capsaicin (Fig. 1A). Capsaicin-evoked toxicity was concentration dependent with half-maximal death occurring in the high nanomolar range (data not shown), consistent with established dose-response profiles in mammalian cells (Gunthorpe et al., 2000; Jerman et al., 2000; Oh et al., 1996). In contrast, capsaicin did not change the viability of a strain harboring a Kir2.1 inward

rectifier K⁺ channel (Minor et al., 1999) (Fig. 1A), suggesting that capsaicin-evoked toxicity is mediated by TRPV1 and is not simply an artifact of expressing a foreign cation channel. Along these lines, we found that lethality was fully suppressed by a TRPV1 pore blocker, ruthenium red (10 μM) (Fig. 1A), or significantly attenuated by an inverse agonist, capsazepine (50 μM) (data not shown). We have previously described a hypersensitive TRPV1 mutant in which an inhibitory C-terminal putative PIP₂ binding module has been deleted, leading to activation at sub-threshold agonist concentrations or ambient temperatures (Prescott and Julius, 2003). Consistent with such functional properties, we found that expression of this potentiated mutant (TRPV1 Δ777-820) was lethal to yeast even in the absence of capsaicin, but growth was restored to wild type levels in the presence of ruthenium red (Fig. 1B). Furthermore, we found that the lethality of capsaicin was augmented when the yeast medium was supplemented with higher levels of sodium (data not shown), suggesting that, as in mammalian cells, toxicity stems from a rise in intracellular cation concentrations to intolerable levels.

Our growth assay demonstrates that sustained TRPV1 activation produces similar long-term effects on survival of yeast and metazoan cells. Furthermore, activation of TRPV1 in yeast by thermal or chemical stimuli occurs on a physiologically relevant time scale, shown by visualizing TRPV1-mediated cobalt accumulation as a direct, short-term assay of channel activity. Stimulus-dependent uptake of cobalt chloride into TRPV1-expressing cells is observed following addition of ammonium sulfide, which generates a readily visible black cobalt sulfide precipitate (Winter, 1987; Wood et al., 1988). In TRPV1-expressing yeast, pellets from non-stimulated cells appeared off-white, but became deep black within five minutes of capsaicin treatment (Fig. 1C), yielding a dose-response relationship consistent with previous functional assays (EC₅₀ ~ 70 nM) (Fig. 1D). As in the cell death assay, Kir2.1-transformed cultures did not respond to capsaicin, and

capsaicin stimulation of TRPV1 in absence of cobalt produced no color change. Similarly, TRPV1-expressing yeast responded robustly to a rise in bath temperature in a manner that closely parallels heat-evoked channel activation in electrophysiological studies (Fig. 1C, E) (Caterina et al., 1997; Tominaga et al., 1998). Thus, our cobalt uptake assay illustrates that TRPV1 forms functional channels in yeast that are reminiscent of native or cloned channels expressed in vertebrate cells.

Unbiased Forward Genetic Screen Reveals Gain-of-Function Mutations

Constitutively active TRPV1 mutants might harbor deficits in some aspect of channel activation, and a comprehensive list of such mutations could provide valuable information about the location of the channel gate. We used the activity-dependent death phenotype described above to identify such TRPV1 alleles which, unlike the wild type channel, conferred significant toxicity even under basal conditions (i.e., in the absence of capsaicin at 30°C). To execute this screen, we introduced a library of randomly mutagenized TRPV1 cDNAs into yeast and plated transformants onto medium containing ruthenium red, thereby blocking TRPV1 to allow for growth of all cells independent of channel activity. Resulting colonies were replica plated onto medium lacking ruthenium red to unmask the lethality of any constitutively active channels (Fig. 2A). Colonies showing reduced survival in the absence of ruthenium red were picked from the original plate and retested to confirm their phenotype.

From this screen, we recovered TRPV1 alleles showing a range of toxic effects (Fig. 2B). Out of approximately 46,000 clones examined, 46 reproducibly exhibited growth impairment in the absence of ruthenium red, yielding an overall hit rate of 0.1% (Table 1). This is in reasonable agreement with the hit rate obtained from a luminometry-based screen for gain-of-function alleles in the yeast TRP channel Yvc1p (Su et al., 2007; Zhou

et al., 2007), and is consistent with the general principle that gain-of-function mutations in channels are rare. Our set of TRPV1 gain-of-function alleles defined a total of 30 unique mutations at 25 amino acid positions (Table 2). Interestingly, recovered mutations were clustered within the presumptive pore and cytoplasmic termini (Fig. 2C). Only two gain-of-function mutations were recovered within the first four transmembrane domains, even though sequencing of randomly selected library clones showed equal mutagenic frequency throughout the coding region. Given the architectural similarity between TRP and voltage-gated channels and the critical role played by the first four transmembrane helices in voltage sensitivity, we were surprised to observe a relative paucity of gain-of-function alleles within this module.

Electrophysiological analysis reveals a range of functional alterations

We used electrophysiological methods to directly characterize the functional properties of mutant channels when expressed in *Xenopus* oocytes. For all channels, basal and proton-evoked currents were assessed at pH 7.4 and 6.4, respectively, and normalized to a saturating concentration (10 μ M) of capsaicin. As expected, wild type TRPV1 responded strongly to capsaicin, but displayed negligible current under basal conditions or in response to pH 6.4 (Fig. 3A), which is just at the threshold concentration required for proton-evoked activation at room temperature (Chuang et al., 2001; Jordt and Julius, 2002; Tominaga et al., 1998). In contrast, eight of the recovered mutants displayed a significant response to pH 6.4, although no basal current was detected at pH 7.4 (Fig. 3B, E). We labeled such mutants as “potentiated.” Furthermore, a second group of mutants displayed a more extreme phenotype, manifest as large basal currents at pH 7.4 (\geq 15% of the maximum capsaicin-evoked response) (Fig. 3C, D, E). These basal currents showed characteristic outward rectification and block by ruthenium red,

indicating that they are carried by TRPV1. We refer to these mutants as “constitutively active.”

Among the constitutively active channels, residues K155 and K160 map to a single N-terminal ankyrin repeat domain, while M581T and F640L are in the S5-pore-S6 region (Fig. 2C). Interestingly, the two N-terminal lysine residues have been previously shown to bind cytoplasmic ATP and calmodulin (Lishko et al., 2007). Lysine-to-alanine substitutions at these positions abolish interaction with ATP or calmodulin and reduce tachyphylaxis (the process by which repeated channel stimulation evokes progressively weaker responses), thereby decreasing efficiency of channel closure upon repeated stimulation. These mutants also display hypersensitivity to capsaicin (Lishko et al., 2007). We asked whether the glutamate substitutions identified by our screen are mechanistically equivalent to the previously described alanine substitutions. Indeed, both sets of substitutions led to comparable toxicity in yeast (Fig. 9A) and high basal currents in oocytes (Fig. 9B), presumably reflecting constitutive activity and/or a failure to desensitize. In any case, our independent identification of these mutations validates the ability of the yeast screen to pinpoint functionally significant TRPV1 residues.

In summary, three functionally distinct classes of TRPV1 alleles arose from our screen, ranging from mutations causing little perturbation of basal or stimulus-evoked activity to those causing dramatic constitutive activation. Interestingly, not all mutants arising from the screen exhibit marked electrophysiological phenotypes in oocytes. This disparity could reflect physiological differences between yeast and metazoan systems, such as transmembrane voltage (highly negative in yeast), growth temperature and extracellular pH, or differential expression of regulatory factors. Nonetheless, the screen has clearly

enriched for mutants with heightened agonist sensitivity, consistent with our goal of identifying substitutions rendering TRPV1 constitutively active or hypersensitive.

F640L renders channels hypersensitive to thermal and chemical stimuli

Among the mutants displaying high constitutive activity in oocytes, we focused on F640L for three main reasons. First, F640L displayed the strongest basal channel activation of all mutants examined (Fig. 3C, D), suggestive of a dramatic alteration in TRPV1 function. Second, F640 lies within the presumptive TRPV1 outer pore, a region that remains relatively unexplored with regard to TRP channel gating. Finally, the F640L allele displayed a unique phenotype in regard to basal versus proton-evoked currents, as described in more detail later.

We examined the biophysical properties of the F640L mutant by patch-clamp recording of transfected HEK293 cells. Consistent with its yeast phenotype, the F640L mutant conferred substantial toxicity when expressed in HEK293 cells, characterized by necrotic morphology similar to that observed in cells expressing wild type TRPV1 after prolonged exposure to capsaicin (Caterina et al., 1997) (Fig. 4A, B). Inclusion of ruthenium red (3 μ M) in the culture medium significantly attenuated the death of F640L-expressing cells, permitting electrophysiological analysis.

We examined the sensitivity of F640L mutant channels to chemical and thermal stimuli. Inside-out membrane patches from HEK293 cells expressing wild type TRPV1 showed small but measurable basal activity at room temperature that exhibited strong outward rectification (i.e. negligible inward current at -60 mV), consistent with previous reports (Chuang et al., 2001; Matta and Ahern, 2007). Subsequent challenge of these cells with a saturating dose of capsaicin (10 μ M) elicited a large (approximately 200-fold) induction

of the basal current (Fig. 4C). In contrast, inside-out patches from the F640L mutant routinely displayed large basal currents with a substantial inward component (Fig. 4D). Despite this difference in basal activity, addition of capsaicin at saturating concentrations produced currents of similar magnitude to those evoked in patches containing wild type channels. We found no significant difference in either the single channel conductance or the relative permeabilities for Na⁺, K⁺, and Ca²⁺ ions when comparing wild type and F640L mutant channels (Figure 10), showing that the F640L mutation affects gating rather than permeation properties.

Consistent with a hypersensitive gating mechanism, we found that the F640L mutant displayed a 35-fold leftward shift in the capsaicin dose-response curve compared to the wild type receptor ($EC_{50} = 1.91 \pm 1.26$ and 65.62 ± 4.03 nM, respectively) (Fig. 5A). Interestingly, mutant channels also exhibited a lower Hill coefficient (0.33 ± 0.08 versus 2.06 ± 0.20 for wild type TRPV1), indicative of decreased agonist cooperativity. Importantly, the basal F640L-mediated current was suppressed by the inverse agonist capsazepine (Fig. 5D), demonstrating that the high constitutive activity is not due to an inability of the channel to close. This mutant also exhibited robust currents well below room temperature, corresponding to a dramatic shift in thermal activation threshold (Fig. 5B) which resembles a proton-potentiated response in cells expressing wild type TRPV1 (Jordt et al., 2000; Tominaga et al., 1998). Because the basal responsiveness of the F640L mutant was reduced with decreased ambient temperature, the mutant phenotype is unlikely to result from a defect in temperature detection *per se*, but rather from an independent mechanism that more generally affects gating. Our data suggest that the gating machinery remains intact in the F640L mutant, but the equilibrium has shifted to favor the open state.

F640L mimics and occludes proton-mediated channel potentiation

In contrast to all other mutants in the high constitutive activity group, only the F640L basal currents were not further potentiated under low pH conditions (Fig. 3E). Nonetheless, addition of capsaicin to F640L-expressing cells led to a marked increase in current, demonstrating that F640L channels are not maximally open in the basal state (Fig. 3C, 4D). As such, the failure to observe proton-evoked potentiation likely reflects a perturbation in the gating mechanism through which protons exert their physiological regulatory effect on TRPV1.

In mammalian cell patch-clamp experiments, we found that, although the wild type channel was potentiated by exposure to pH 6.2, the F640L current was completely unaffected under these conditions (Fig. 5C-E), demonstrating a defect in proton-evoked potentiation. We also observed that a weakly alkaline solution (pH 8.2) failed to reduce the F640L-mediated basal current, even though the same conditions suppressed currents evoked by a moderate dose of capsaicin (70 nM) in cells expressing the wild type channel (data not shown). However, higher doses of protons could activate the F640L mutant in a manner similar to the wild type channel ($\text{pH}_{50} = 5.60 \pm 0.03$ versus 5.72 ± 0.19 for wild type and F640L mutant channels, respectively), illustrating that while the mutant has lost the ability to be potentiated within a certain pH range, its proton activation has not been completely ablated.

Taken together, our data show that the F640L mutation enhances sensitivity to heat and capsaicin by shifting the stimulus-response relationships of the channel leftward, while also decreasing apparent cooperativity of gating. Indeed, this phenotype closely resembles that of wild type TRPV1 channels operating under acidic conditions. In

contrast, the sensitizing effects of extracellular protons are lost in the F640L channel, as one might expect if this mutation phenocopies the proton potentiated state.

Additional substitutions in the outer pore alter TRPV1 gating

The F640 residue is located near the C-terminal end of a 15 amino acid stretch immediately preceding the presumptive selectivity filter, a region known in K⁺ channels as the pore helix (Doyle et al., 1998). While TRP and K⁺ channels share limited homology, computer algorithms (Jones, 1999) predict a high degree of helicity in this region of TRPV1, suggesting that a pore helix may indeed be present (Fig. 6A). While it is generally accepted that the outer pore region contains structural determinants for ion permeation and block (Yellen, 1998), the role of pore helices in the regulation of channel gating has been less fully explored. Our yeast screen and functional characterization of F640L suggest that the pore helix may be a particularly critical for TRPV1 gating.

We randomized the F640 codon to fully explore the structural requirements at this position (Fig. 6B). Transformants from a F640 mini-library were evaluated for wild type, gain of function, or loss-of-function behavior using the yeast growth assay. Most substitutions at this position, particularly those of a hydrophilic nature, weakened or abolished channel activity. In contrast, several hydrophobic amino acids supported wild type functionality, except for leucine and isoleucine, which produced constitutively active channels. Thus, our codon randomization illustrates that most hydrophobic substitutions at F640 produce functional channels whereas two small hydrophobic residues support constitutive channel activity, suggesting that F640 is buried in a non-polar environment.

Although we analyzed a large number of clones in our initial yeast screen, it is possible that some function-altering substitutions went undetected. We therefore screened a

more restricted yeast library in which only the TRPV1 pore helix and its immediate environment (residues 626-660) were randomly mutagenized to uncover additional substitutions in this region that might lead to constitutive activation (Table 1). We uncovered nine additional substitutions conferring a toxic phenotype in yeast. Of these, two (N628D and V658A) showed a potentiation effect under moderately acidic conditions, while two more (T641S and T650S) showed high basal activity (Fig. 6C, D). Interestingly, T641S (and, to a lesser extent, T650S) mutants displayed large constitutive channel activation with relative insensitivity to pH 6.4. The T641S mutant also caused widespread death in HEK293 cells (data not shown). Thus, at least two mutants recovered in the outer pore region are reminiscent of the original F640L mutation. Because substitutions in two adjacent residues (F640 and T641) produce similar functional alterations, we conclude that the short stretch of amino acids at the interface between the pore helix and the permeation pathway forms a particularly crucial part of the gating apparatus.

The functional role of the pore helix is conserved in related TRP family members

Mammalian TRPV channels are highly divergent at the amino acid level. Rat TRPV1, TRPV2, TRPV3, and TRPV4 exhibit only 21% identity overall, while TRPV5 and 6 are even more distantly related. Interestingly, the 13 residue-long stretch connecting the pore helix and selectivity filter displays 69.2% identity in TRPV1 – 4 (Fig. 6A), suggesting that some TRP channels may share common architectural features within this region. We therefore asked whether any pore helix mutations identified in our TRPV1 screen would produce a gain-of-function effect in other TRPV family members.

TRPV3 is activated by warm temperatures, with a threshold in the 33°C - 38°C range (Peier et al., 2002b; Smith et al., 2002; Xu et al., 2002). Sequence alignments reveal a

threonine at position 636 in TRPV3 corresponding to T641 in TRPV1 (Fig. 6A). We asked whether TRPV3 T636S channels displayed constitutive activity similar to TRPV1 T641S. Strikingly, transfection of TRPV3 T636S into HEK293 cells produced massive cell death that was significantly attenuated by ruthenium red, while no toxicity was observed from the wild type channel (Fig. 7D). In inside-out patches excised from oocytes expressing wild type TRPV3, we observed small outwardly rectifying basal currents that were robustly stimulated by the broad spectrum TRP channel agonist 2-aminoethoxydiphenyl borate (2-APB) (Chung et al., 2004a; Hu et al., 2004) (Fig. 7A). In contrast, TRPV3 T636S exhibited large basal currents characterized by high channel noise and outward rectification (Fig. 7B), reminiscent of wild type TRPV3 activity at warm temperatures. As with the TRPV1 pore helix mutant, TRPV3 T636S channels showed substantial basal currents at negative holding potentials. By normalizing the basal currents to a maximal 2-APB-evoked response (300 μ M), we estimate that T636S displays approximately 300-fold increase in spontaneous activity compared to the wild type channel (Fig. 7C). TRPV3 T636S basal currents were suppressed by cold (10°C), and the inward current was strongly attenuated by ruthenium red (Fig. 7A-B, and data not shown), a pharmacology consistent with TRPV3-evoked currents in native or heterologous systems (Chung et al., 2004b; Peier et al., 2002b; Smith et al., 2002; Xu et al., 2002). We also investigated the effects of an F603L substitution in TRPV2, a position corresponding to F640L in TRPV1. Unlike other TRPV channels, wild type TRPV2 exhibits no measurable basal activity when heterologously expressed, and we did not detect basal currents from either wild type or F603L TRPV2 channels (data not shown). Nevertheless, we observed that the F603L mutant displays enhanced 2-APB sensitivity (Fig. 7E, F). Taken together, our data show that mutations in pore helices shift multiple TRPV channels into an open conformation, showing that this region plays a conserved role in gating of different TRP family members by diverse chemical and thermal stimuli.

DISCUSSION

Conservation of TRPV1 functional properties in a non-mammalian genetic system

Spontaneous gain-of-function mutations have provided valuable insights into ion channel permeation and gating (Kohda et al., 2000; Navarro et al., 1996). While naturally occurring mutations have been identified in mammalian TRP channels (Asakawa et al., 2006; Kim et al., 2007; Xu et al., 2007), these sporadic genetic events are too rare to support a systematic analysis of TRP channel functionality. Here we report a facile and unbiased forward genetic screen for isolating gain-of-function mutations in a mammalian TRP channel based on a simple yeast growth phenotype. This high-throughput methodology enabled us to survey the TRPV1 coding region for substitutions that cause constitutive activation. Such an approach has been applied to microbial cation channels (Loukin et al., 1997; Ou et al., 1998) and vertebrate inward rectifier K⁺ channels (Sadjja et al., 2001; Yi et al., 2001), and we now extend this strategy to include non-selective mammalian cation channels. Previous studies have exploited polymorphisms between TRP channel homologues or orthologues to delineate molecular determinants underlying ligand activation (Chuang et al., 2004; Jordt and Julius, 2002; Ryu et al., 2007), but this methodology is limited for numerous reasons. TRP channel subtypes generally exhibit low sequence homology and thus channel chimeras are often non-functional. In addition, such an approach cannot pinpoint residues that are conserved across channels. Indeed, many mutations uncovered by our screen are highly conserved in TRPV1 orthologues or other TRPV family members, attesting to the increased power of this approach for detecting core structural elements. A select percentage (0.10%) of mutant channels emerged from the cell death assay, of which ~40% showed *bona fide* functional perturbations when examined in vertebrate expression systems, attesting to both the

stringency and efficiency of the screen. Perhaps most importantly, this screen revealed a number of interesting channel mutants that have not been described in previous structure-function studies.

Remarkably, rat TRPV1 expressed in yeast recapitulates functional properties observed in neurons or other mammalian cell types, including sensitivity to noxious heat and capsaicin. This suggests that both chemical and thermal sensitivity are intrinsic channel properties, not requiring membrane or cytoplasmic factors specific to metazoans. Moreover, yeast are hyperpolarized compared to metazoan cells, with membrane potentials estimated at -100 to -250 mV (Serrano and Rodriguez-Navarro, 2001). The observation that TRPV1 can be robustly activated in yeast therefore favors a modest role for membrane voltage as a regulator of channel gating (Latorre et al., 2007; Matta and Ahern, 2007).

The pore helix as a transducer of TRPV1 gating

A hallmark of many TRP channels is their ability to integrate multiple physiological inputs (Clapham, 2003; Dhaka et al., 2006; Julius, 2005; Venkatachalam and Montell, 2007). This is exemplified by TRPV1, whose role as a polymodal detector of chemical and physical stimuli underlies its capacity to regulate sensory neuron excitability under normal and pathophysiological conditions (Tominaga et al., 1998). Different TRPV1 stimuli (e.g. capsaicin, heat, acidic pH) produce synergistic effects on channel activation, while antagonists (e.g. capsazepine, cold, alkaline pH) diminish responses to multiple activating stimuli, providing evidence for crosstalk and convergence in channel gating mechanisms (Tominaga et al., 1998). This is consistent with our observation that the F640L mutant shows a shallowing of dose-response profiles to capsaicin and temperature, accompanied by a leftward shift in activation thresholds. This decreased

cooperativity and increased sensitivity suggest that the pore helix region undergoes a structural transition common to all activating modalities, for which the energetic barrier is lowered by mutations such as F640L.

In the case of extracellular protons, it is possible to separate their ability to potentiate other stimuli under moderately acidic (pH 6.4) conditions versus their ability to activate TRPV1 *de novo* at room temperature (pH < 6.0). Mutations at two extracellular glutamate residues, E600 or E648, selectively alter the modulatory versus activating effects of protons, respectively (Jordt et al., 2000). In this regard, it is interesting that F640L displays agonist hypersensitivity and loss of proton-mediated potentiation, but shows normal *de novo* gating by protons, similar to positively charged substitutions at E600 (Jordt et al., 2000). Thus, perturbations in the pore helix are sufficient to favor an open conformation, perhaps mimicking and occluding the modulatory effect mediated by interaction of protons with extracellular sites such as E600.

While our data establish a role for the pore helix in proton-mediated potentiation, recent work suggests that this domain may also be involved in *de novo* proton gating. Mutation of residue T633 in TRPV1, also located within the pore helix, abolishes proton-evoked activation, although protons can still potentiate currents evoked by capsaicin (Ryu et al., 2007). Thus, other pore helix substitutions show a distinct but related phenotype to that observed in our study, namely, alteration of *de novo* proton-evoked activation rather than proton-mediated potentiation. These studies support the general conclusion that conformational changes in the pore helix are critical for both the activating and modulatory effects of protons on TRPV1, and underscore the idea that, while proton-mediated potentiation and *de novo* activation are determined by distinct sets of residues, their effects on channel gating both involve the pore helix as a key regulatory domain.

Based on secondary structure predictions and their relationship to known K⁺ channel structures, E600 and E648 are predicted to lie near the extracellular face of the outer pore, close to the top of the pore helix (Fig. 8), and it is conceivable that protonation of these residues could induce conformational rearrangements propagating through the pore helix that ultimately lead to channel opening. Perhaps the C-terminus of the pore helix forms a movable barrier to ion flux, either by protruding directly into the permeation pathway or by constricting the selectivity filter into a nonconductive conformation similar to that observed in one crystal structure of the prokaryotic K⁺ channel KcsA (Zhou et al., 2001). Alternatively, residues within the pore helix might not form a physical occlusion *per se*, but rather stabilize an open conformation of the channel, comparable to a model proposed for the gating of inward rectifier K⁺ channels (Alagem et al., 2003).

The pore helix as a conserved element in TRP channel gating

Our present analysis of the pore helix suggests that its role in gating is conserved in at least a subset of TRP channels. We found that mutation of pore helix residues leads to constitutive activation of TRPV3, as well as potentiation of TRPV2. Therefore, our study suggests that the pore helix plays a general role in TRP channel gating that has not been previously appreciated. TRPV1 may represent a case in which a universal gating element has been usurped to serve as an allosteric regulatory site for protons, allowing for alteration of TRPV1 sensitivity in the setting of inflammation and tissue acidosis. Thus far, relatively few structural elements have been shown to play conserved functional roles in TRP channels, and it may be worthwhile to investigate pore helices as gating elements in other mammalian TRP family members.

While numerous studies have localized the molecular determinants of ion permeation and block to the outer pore region of TRP (Voets et al., 2004; Voets et al., 2002) and other cation channels (Ahern et al., 2006; Chatelain et al., 2005; Doyle et al., 1998), the role of the pore helix in TRP channel gating and agonist sensitivity is unexpected. Indeed, structural analyses suggest that voltage activation of K⁺ channels involves alteration of interactions between the S4-S5 linker and the cytoplasmic end of S6, relieving strain on the helical bundle crossing that forms the intracellular gate (Long et al., 2005a, b; Tombola et al., 2006). In this model, the outer pore region is an ion conduit that remains relatively stationary during the overall gating transition. On the other hand, the outer pore is known to play a critical role in the context of C-type inactivation, the process by which repetitive voltage stimulation desensitizes voltage-gated K⁺ channels via a mechanism involving collapse of the selectivity filter. Mutations in the outer pore region, including the pore helix, can dramatically influence the extent of K⁺ channel C-type inactivation, suggesting that these regions play an important role in modulating the biophysical properties of open K⁺ channels (Cordero-Morales et al., 2006; Hoshi et al., 1991; Kiss and Korn, 1998; Liu et al., 1996; Lopez-Barneo et al., 1993). Thus, the outer pore can influence the level of K⁺ channel activity under certain conditions.

Aside from K⁺ channels, additional studies have suggested a role for the pore helix in gating of other 6TM channels. Cysteine accessibility experiments in CNG channels (Liu and Siegelbaum, 2000), as well as in TRPV5 and TRPV6 (Voets et al., 2004; Yeh et al., 2005), show that residues in the pore helix are differentially reactive to modifying agents in the closed and open states, illustrating that in these cases (and unlike K⁺ channels), the pore helix may rotate during gating. Together with our findings, these observations indicate that, despite topological resemblance to voltage-gated K⁺ channels, gating of other members of the 6TM superfamily may involve a conformational change in the outer

pore region. This is not to say that the structural determinants of activation identified in voltage-gated channels are irrelevant to TRP channels. Indeed, recent work has identified spontaneous dominant mutations in TRPV3 linked to hair loss and atopic dermatitis that dramatically enhance basal activity when engineered into the cloned channel (Asakawa et al., 2006; Xiao et al., 2007). Interestingly, both mutations map to a single residue in the putative S4-S5 region of TRPV3, suggesting that conformational changes in this linker might also play a role as molecular determinants of channel activation, perhaps via interaction with a cytoplasmic activation gate at the intracellular segment of S6. These and other studies highlight the idea that TRP channel gating likely involves multiple regions including the pore helix and the S4-S5 linker. Future work will address the physical and functional interplay between these regions in shaping the physiological properties of TRP channels.

EXPERIMENTAL PROCEDURES

Molecular biology

Rat TRPV1 was cloned into p425GPD. For mutagenic library construction, TRPV1 was amplified using *Taq* polymerase (New England Biolabs) under standard conditions for 25 cycles, and the mutagenized N- or C-terminal cassettes separately reintroduced back into the wild type construct to generate two distinct libraries with the desired mutagenesis frequency. For the pore helix library, mutagenesis rate was boosted by supplementing the PCR with MgCl₂ and MnCl₂ (final concentrations of 7 and 0.5 mM, respectively), increasing cycle number to 40, and decreasing concentration of dATP and dGTP relative to dCTP and dTTP. Site-directed mutagenesis was performed by overlap extension PCR or QuikChange (Stratagene), or by yeast *in vivo* recombination. Mutant

channels were cloned into the mammalian/oocyte expression vector pMO (gift of Lily Jan) for functional analysis. All constructs were verified by DNA sequencing.

Yeast transformation and replica plating

Strain BY4741 (*Mata his3Δ1 leu2Δ0 met15Δ0 ura3Δ0*) was transformed with lithium acetate/polyethylene glycol and selected on medium lacking leucine. Media was supplemented with 20 mM MES and buffered to pH 6.2, under which conditions little or no inward current is observed in mammalian cells expressing TRPV1 (Figure 5C). Capsaicin (Tocris) and/or ruthenium red (Sigma) were added to molten agar prior to pouring. After two days growth on selective medium with 3 μM ruthenium red (mother plate), transformants were replica plated onto two plates, one lacking and another containing 10 μM ruthenium red (daughter plates), the latter designed to eliminate false positives arising from inefficient colony transfer from the mother plate. After two more days, the daughter plates were aligned to identify clones exhibiting basal toxicity. Clones from this first round of screening were retested by serial dilution. Plasmids were subsequently rescued and retransformed into fresh BY4741 to confirm the phenotype.

Cobalt uptake assay

Yeast cultures were grown to mid-log phase in selective medium and washed once in cobalt uptake assay buffer (in mM: 58 NaCl, 5 KCl, 2 MgCl₂-6H₂O, 0.75 CaCl₂, 12 glucose, 137 sucrose, 10 HEPES, pH 7.4). Pellets were resuspended in assay buffer with 5 mM CoCl₂ plus varying concentrations of capsaicin and incubated for 5 min at 30°C. For temperature experiments, cells were subjected to varying temperatures for five minutes using a gradient PCR thermocycler (MJ Research). Cells were washed twice in assay buffer and stained with 1% (NH₄)₂S.

Mammalian cell culture and electrophysiology

HEK293T cells were cultured and transfected as previously described (Chuang et al., 2004.) For some experiments, we generated stable tetracycline-inducible Flp-in T-rex HEK293 cell lines (Invitrogen) expressing wild type TRPV1 or the F640L mutant. For whole-cell or excised patch recordings, bath solution contained (in mM): 140 NaCl, 10 HEPES, 1 MgCl₂-6H₂O, 1 EGTA, pH 7.4. Pipette solution was identical, except that CsCl was substituted for NaCl. For proton experiments, we substituted MES for HEPES in the bath and adjusted pH accordingly. For single channel analysis, pipette solution contained 1 μM capsaicin. Relative permeabilities were estimated from reversal potential shifts between solutions containing (in mM): 10 HEPES, 10 glucose, and either 140 NaCl, 140 KCl, or 125 NMDG-Cl + 10 CaCl₂. Liquid junction potentials did not exceed 3 mV. Pipettes were fabricated from borosilicate glass (WPI) with resistances after fire-polishing of 1-2 MΩ for whole-cell experiments, 0.8-1.2 MΩ for inside-out macropatch experiments, and 6-10 MΩ for cell-attached single channel experiments. Currents were recorded with an Axopatch 200B amplifier (Molecular Devices) using a 180 ms voltage ramp from -120 mV to +80 mV delivered once per second. Currents were recorded at 5 kHz, filtered at 2 kHz, and analyzed with pClamp 10 (Molecular Devices). Temperature ramps were generated with a custom-made Peltier device (Reid-Dan Electronics). Capsaicin, capsazepine, and 2-APB were dissolved in DMSO, and ruthenium red was dissolved in water. Drugs were diluted into recording solution immediately prior to experiments.

Xenopus oocyte culture and electrophysiology

Surgically extracted oocytes from *Xenopus laevis* (Nasco) were cultured and analyzed 2-14 days post-injection by TEVC as previously described (Chuang et al., 2004). For proton experiments, MES was substituted for HEPES and pH adjusted accordingly. For

patch clamp analysis, both the bath and pipette solutions contained (in mM): 140 CsCl, 10 HEPES, 1 MgCl₂-6H₂O, 1 EGTA, pH 7.4. Macropatches were excised from devitellinized oocytes using pipettes with resistances of 0.3-0.8 MΩ and currents were analyzed as described for mammalian cell patch clamp.

Mammalian cell death assays

After 16 hours, transfected HEK293 cells were stained with DAPI (500 ng/ml) to identify dead cell nuclei. DAPI-positive cells were averaged from four different fields per transfection. Each field contained approximately the same total number of cells.

Figure 1

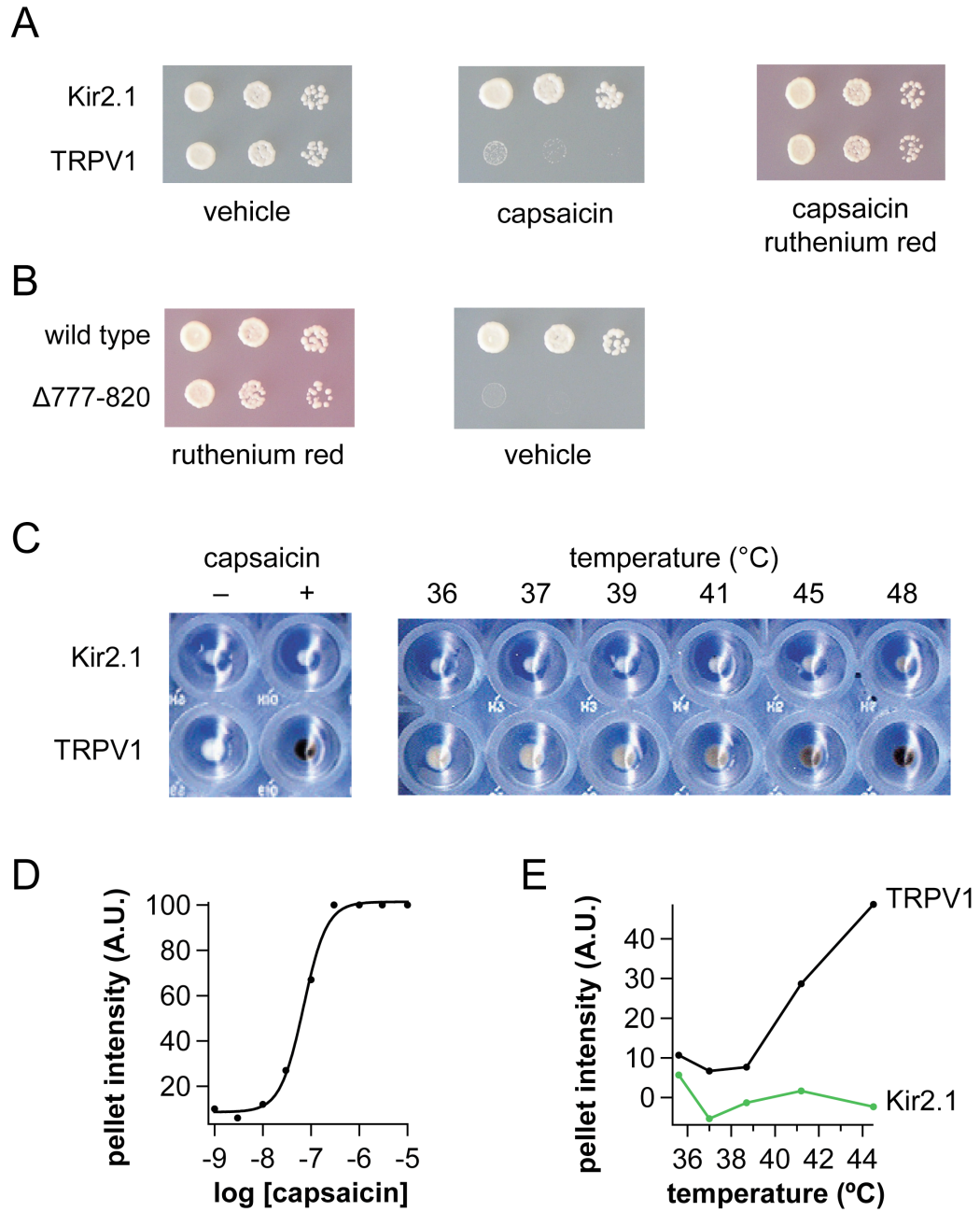


Figure 1 Mammalian TRPV1 forms functional channels in yeast

(A) Serial dilution assay for growth of yeast strains transformed with plasmids encoding mouse Kir2.1 or rat TRPV1. Yeast were resuspended to approximately the same density, spotted (from left to right) on indicated media and allowed to grow at 30 °C for 3 days. (B) Serial dilution assay for wild type TRPV1 versus TRPV1 $\Delta 777-820$, grown as described in (A). (C) Representative cobalt uptake assay performed with yeast expressing TRPV1 or Kir2.1. Cells were exposed to 10 μM capsaicin (at 30°C) or elevated bath temperature (36-48°C) and cobalt accumulation visualized in cell pellets collected in microtiter wells. (D) Intensity of cobalt sulfide staining was determined using pixel quantitation (arbitrary units), yielding a capsaicin concentration response relationship that could be fit with a sigmoid function. (E) Quantitation of TRPV1 (black) or Kir2.1 (green) temperature responsiveness in yeast using the cobalt uptake assay, revealing a TRPV1 thermal activation threshold near 40°C.

Figure 2

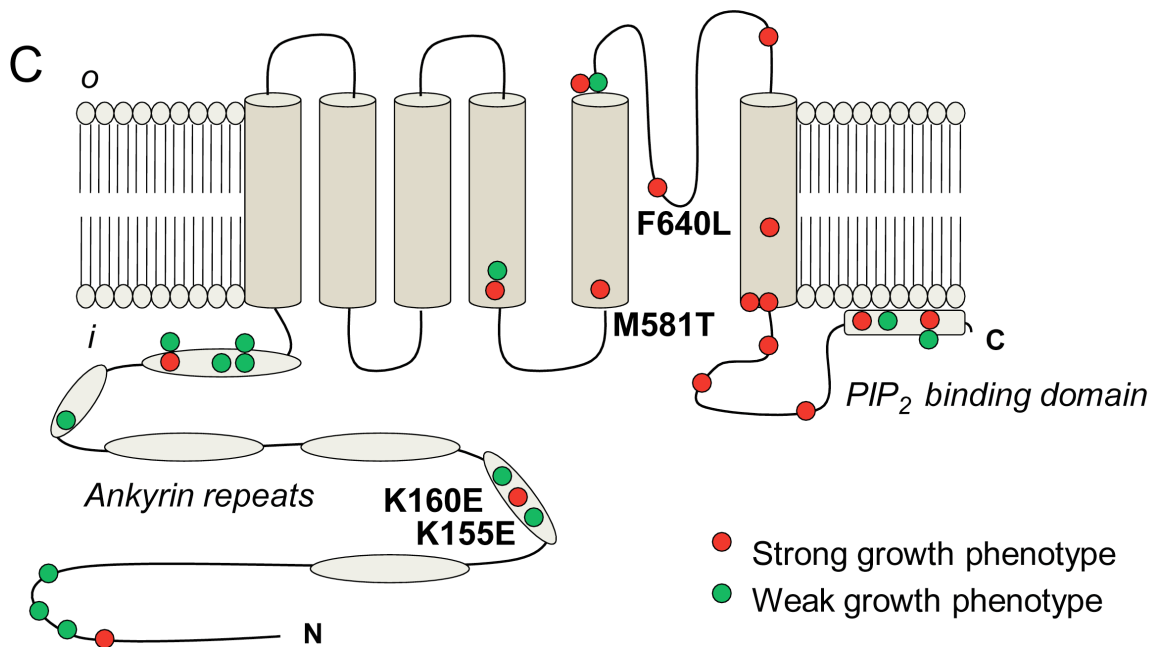
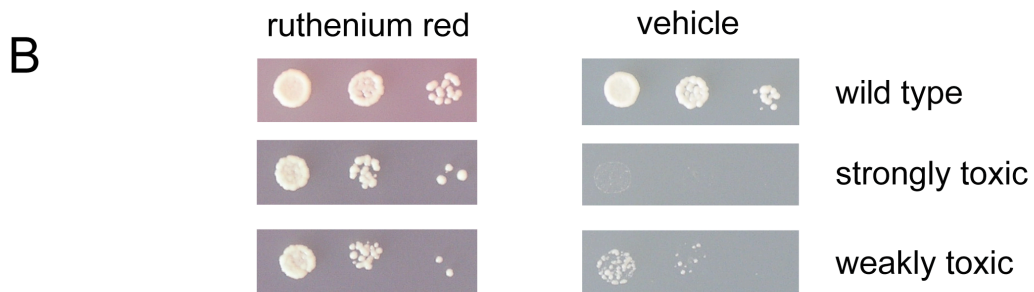
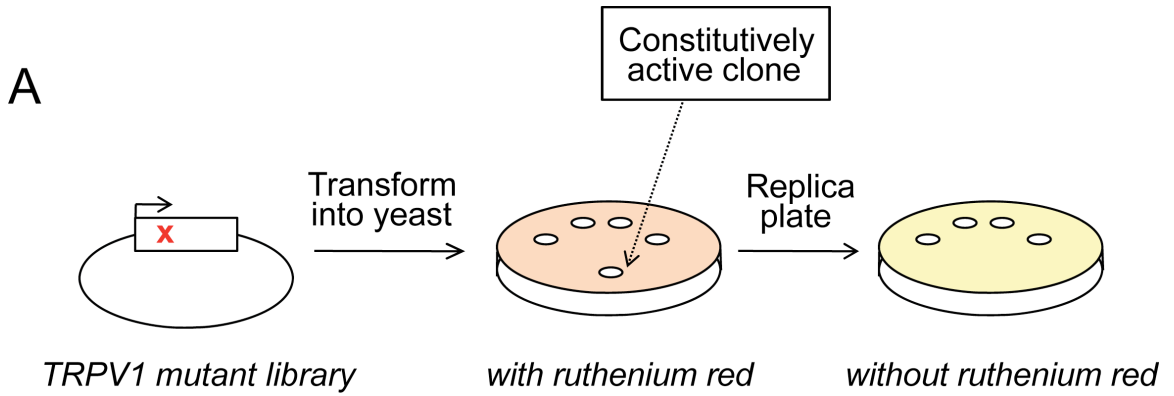


Figure 2 Yeast genetic screen identifies gain-of-function TRPV1 alleles

(A) Outline of the screening procedure: yeast were transformed with the randomly mutagenized TRPV1 library and grown for 2 days following replica plating. Subsequently, toxic alleles were identified and picked from the ruthenium red plate for secondary analysis and plasmid rescue. (B) Serial dilution assays of cultures expressing wild type TRPV1 or representative mutants illustrating the range of toxic phenotypes recovered from the yeast screen. (C) Each allele recovered in the screen was mapped onto a topology diagram of TRPV1. Red or green spheres indicate location of mutations causing strong or weak toxic phenotypes, respectively. N-terminal ankyrin repeats, transmembrane helices (S1-S6), and putative C-terminal PIP₂ binding domain are shown. Mutants exhibiting high constitutive activity in electrophysiological assays (see figure 3) are labeled for reference.

Figure 3

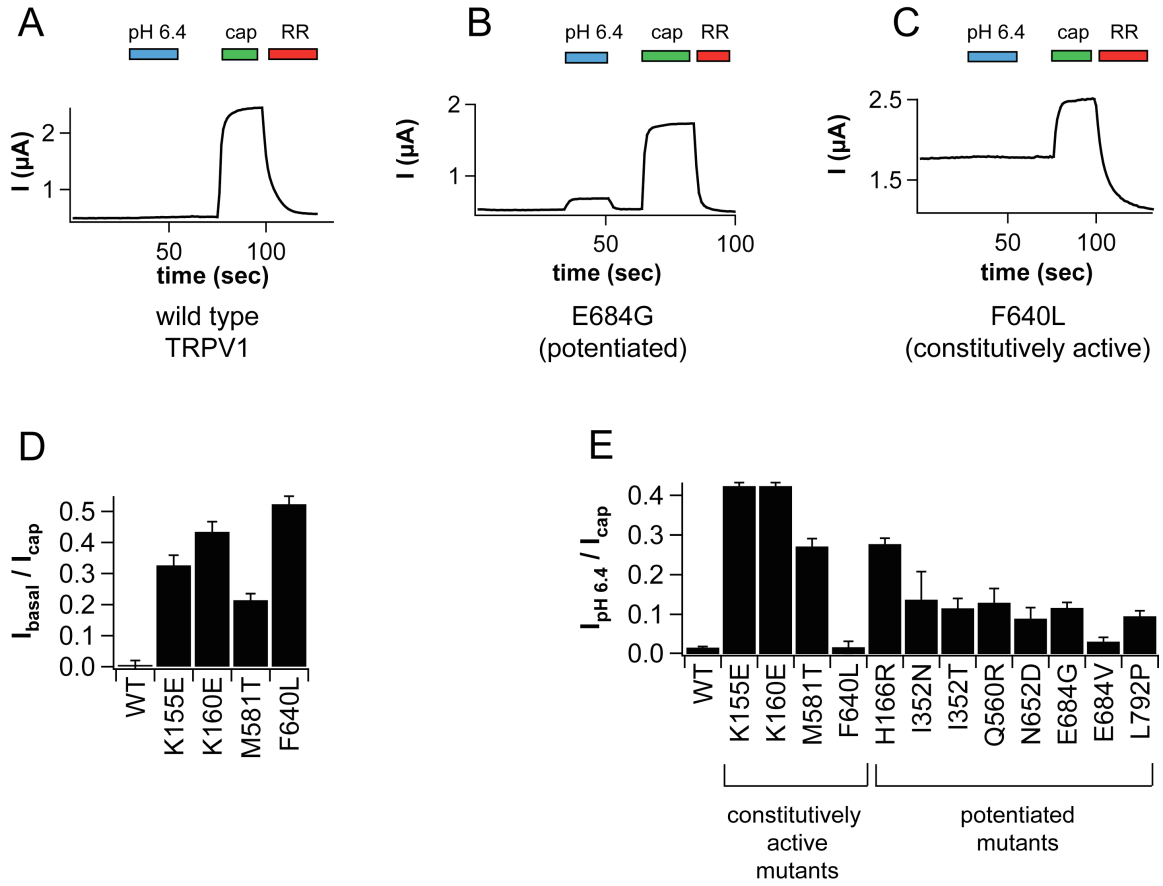
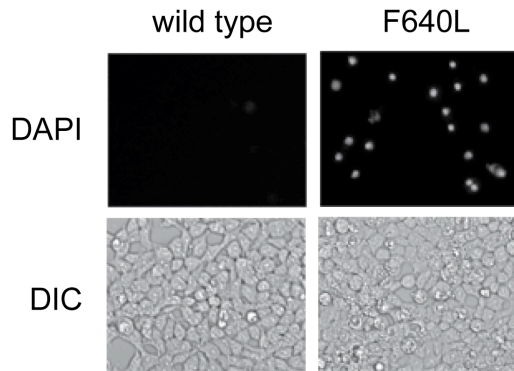


Figure 3 Mutants recovered from the yeast screen display altered electrophysiological properties

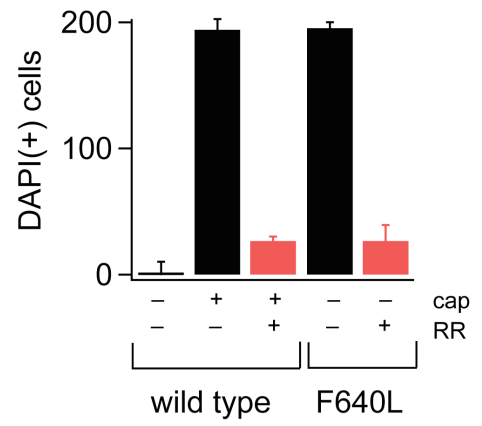
Representative current traces from two-electrode voltage clamp (TEVC, +80 mV) recordings of oocytes expressing wild type TRPV1 (**A**), potentiated mutants (**B**), or constitutive mutants (**C**). Oocytes were challenged with protons (pH 6.4), capsaicin (10 μ M), or ruthenium red (10 μ M). (**D**) Quantitation of basal currents for all TRPV1 mutants exhibiting constitutive activity (normalized to a saturating capsaicin response; mean \pm s.e.m., $n \geq 3$ per construct). Currents in the presence of ruthenium red (10 μ M) were used as baseline. For wild type TRPV1, >90% block of capsaicin-evoked currents was achieved after 30 seconds of ruthenium red treatment, and the wild-type value of $I_{\text{basal}}/I_{\text{cap}}$ was subtracted from all measurements. (**E**) Quantitation of pH 6.4 responses (normalized to a saturating capsaicin response) for all TRPV1 mutants exhibiting constitutive or potentiated activity. Data represent mean \pm s.e.m., $n \geq 3$ per construct.

Figure 4

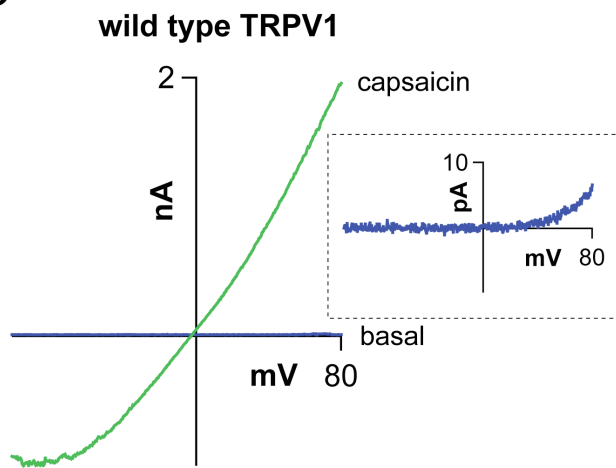
A



B



C



D

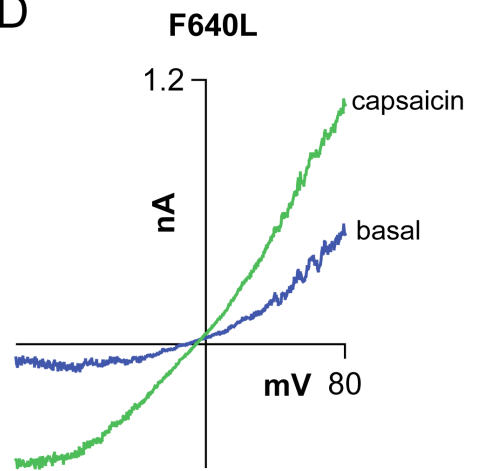


Figure 4 F640L mutant TRPV1 channels are toxic and display high basal activity in mammalian cells

(A) Representative image of HEK293 cells transfected with wild type TRPV1 or F640L mutant after staining with 4',6-Diamidino-2-Phenylindole (DAPI) to identify dead cells. Corresponding differential interference contrast (DIC) images are shown below. **(B)** Quantitation of cell death assay as performed in (A). Black and red bars represent cell death in the absence or presence of ruthenium red (3 μ M, RR), respectively (mean \pm s.e.m.). Death among cells transfected with wild type TRPV1 with or without capsaicin (1 μ M, cap) is shown for comparison. Background cell death was determined from cells transfected with vector alone and subtracted from each measurement. **(C, D)** Representative inside-out patch recording from HEK293 cells transfected with wild type TRPV1 or the F640L mutant. Voltage ramps under basal conditions (blue) or in the presence of 10 μ M capsaicin (green) are shown. Inset: for the wild type channel, 25 consecutive ramp traces were averaged and leak-subtracted to accurately derive the ensemble average basal current.

Figure 5

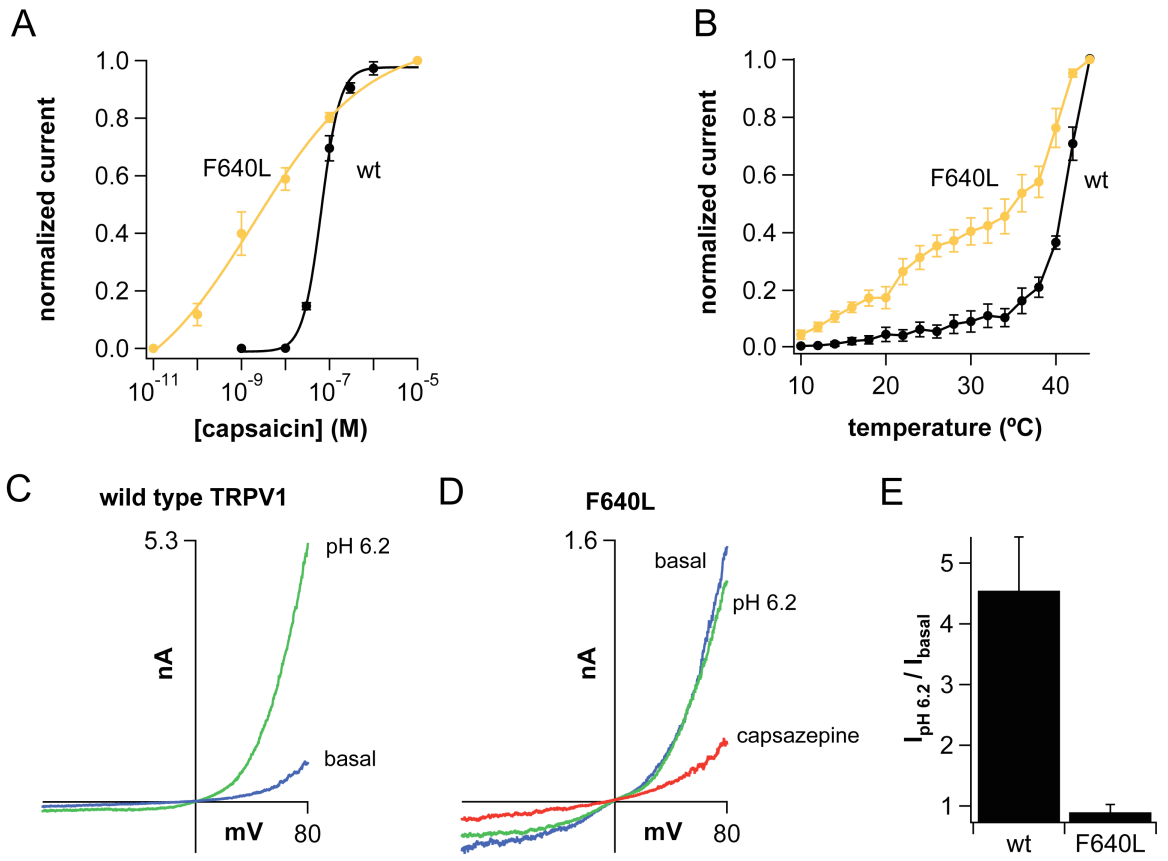


Figure 5 F640L TRPV1 mutant channels show enhanced chemical and thermal sensitivity, but decreased proton potentiation

(A) TEVC recording of TRPV1 wild type (black) or F640L (orange) channels reveals leftward shift in the agonist dose-response relationship (mean \pm s.e.m. at +80 mV, n = 4 oocytes per condition). (B) Inside-out patch recording from HEK293 cells transfected with wild type (black) or F640L (orange) channels stimulated with a temperature ramp from 10 to 44 °C (mean \pm s.e.m. at -60 mV, n \geq 4 patches per condition) reveals hypersensitivity to heat. (C, D) Voltage ramp traces from whole-cell patch clamp recordings of HEK293 cells expressing wild type or F640L mutant channels. Blue traces indicate basal channel current at room temperature in pH 7.4 bath solution, while green traces indicate channel current after perfusion with pH 6.2 bath solution. Subsequent addition of capsazepine (30 μ M, red) efficiently inhibited F640L basal current. (E) Quantitation of fold potentiation (at +80 mV) at pH 6.2 vs. 7.4 for wild type and F640L channels, as in (C) and (D) (mean \pm s.e.m., n = 4 - 6 cells per condition).

Figure 6

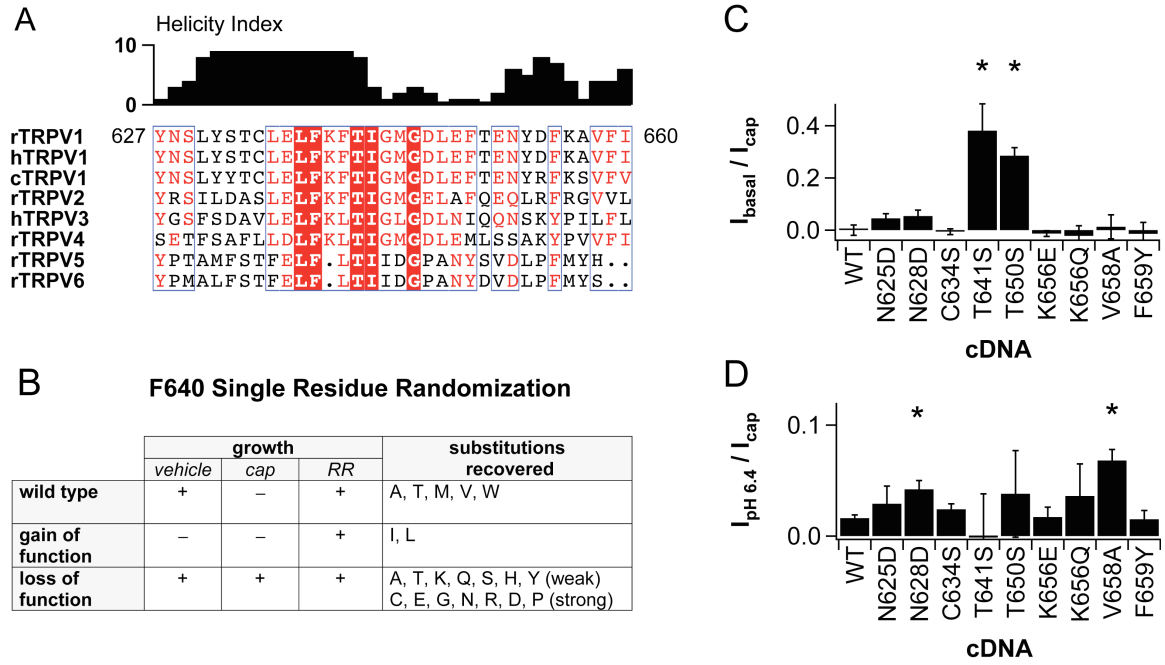


Figure 6 Additional substitutions in the TRPV1 pore helix affect channel activation

(A) Alignment of the pore helices and selectivity filters from various TRPV channels (r = rat, h = human, c = chicken). Helicity index for rat TRPV1 (0-10, generated using PSIPRED) is shown above alignment. (B) Summary of F640 saturation screen. Transformants harboring a library of TRPV1 mutants (with a randomized F640 codon) were scored according to growth pattern and mutant plasmids sequenced to determine the amino acid substitution. Note that F640A and F640T were scored as both “wild type” and “weak loss of function”, consistent with an intermediate phenotype. (C, D) Quantitation of normalized basal or pH-evoked currents for mutants recovered from the pore helix screen, analyzed by TEVC as in figure 3. * $p \leq 0.01$, Student’s t-test.

Figure 7

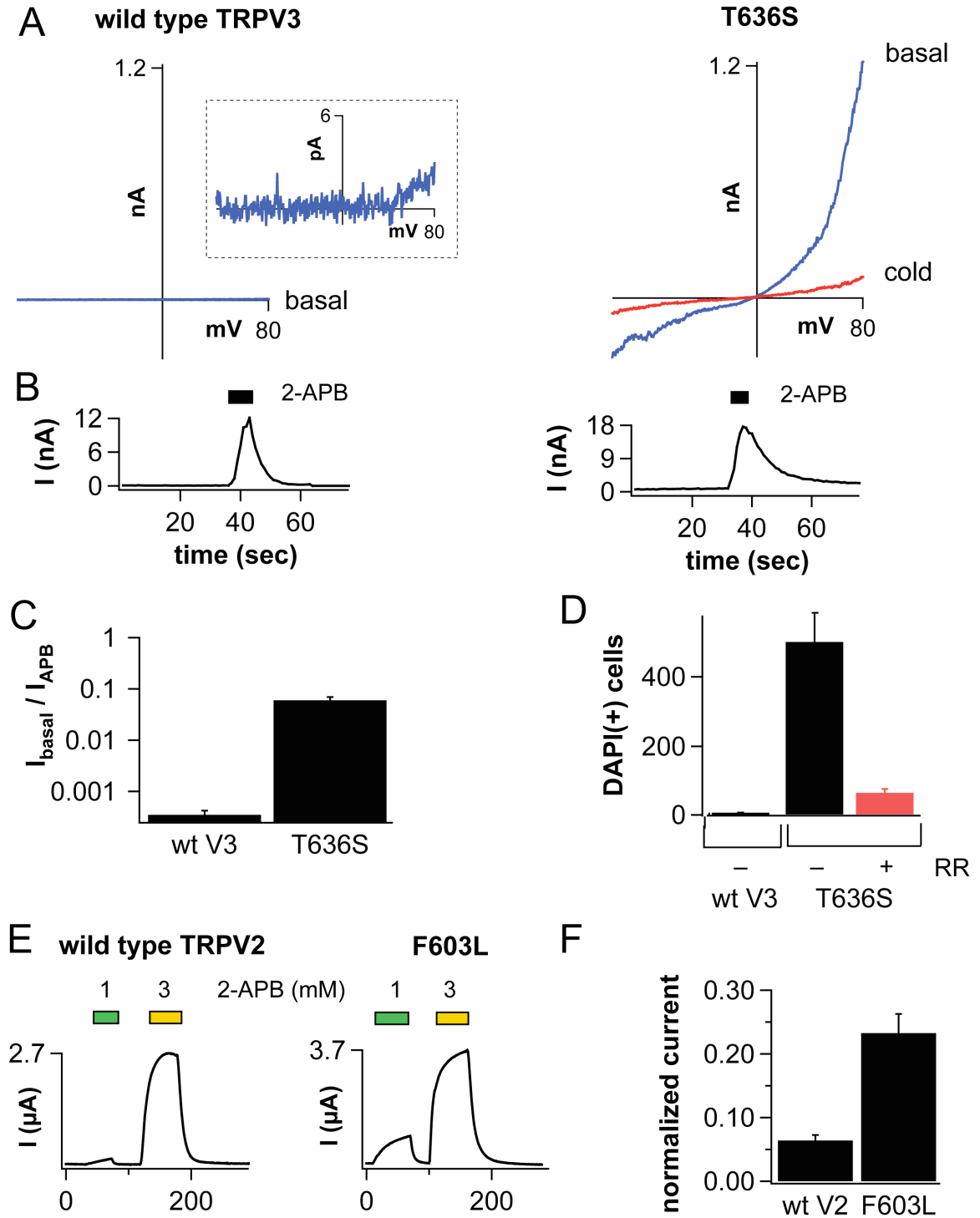


Figure 7 The gating function of the pore helix is conserved across TRPV channels

Voltage ramp traces from representative inside-out macropatches excised from oocytes expressing wild type human TRPV3 (**A**) vs. T636S mutant (**B**). Patches were allowed to stabilize for five minutes after excision. Blue traces indicate basal current at room temperature. Inset represents ensemble average basal current for wild type TRPV3. Red trace shows current at 10°C, illustrating block of T636S basal activity by cold temperature. Corresponding current vs. time plots are shown below each set of voltage ramps, illustrating that wild type and mutant channels respond similarly to 300 μ M 2-APB. (**C**) Quantitation of basal current (normalized to 300 μ M 2-APB response) for TRPV3 wild type or T636S mutant channels ($n \geq 4$ patches per condition). (**D**) TRPV3 T636S mutant caused massive toxicity in transfected HEK293 cells that was blocked by ruthenium red (RR, 3 μ M, red bar). Wild type TRPV3 is shown for comparison. (**E**) Representative traces from TEVC recordings of oocytes expressing wild type rat TRPV2 vs. F603L mutant. Oocytes were exposed to 1 or 3 mM 2-APB (green or yellow bars, respectively). (**F**) Quantitation of 1 mM 2-APB evoked responses in cells expressing wild type TRPV2 or F603L mutant channel (normalized to the 3 mM 2-APB response) reveals that the F603L mutant displays enhanced sensitivity to a lower concentration of 2-APB ($p \leq 0.001$, Student's t-test).

Figure 8

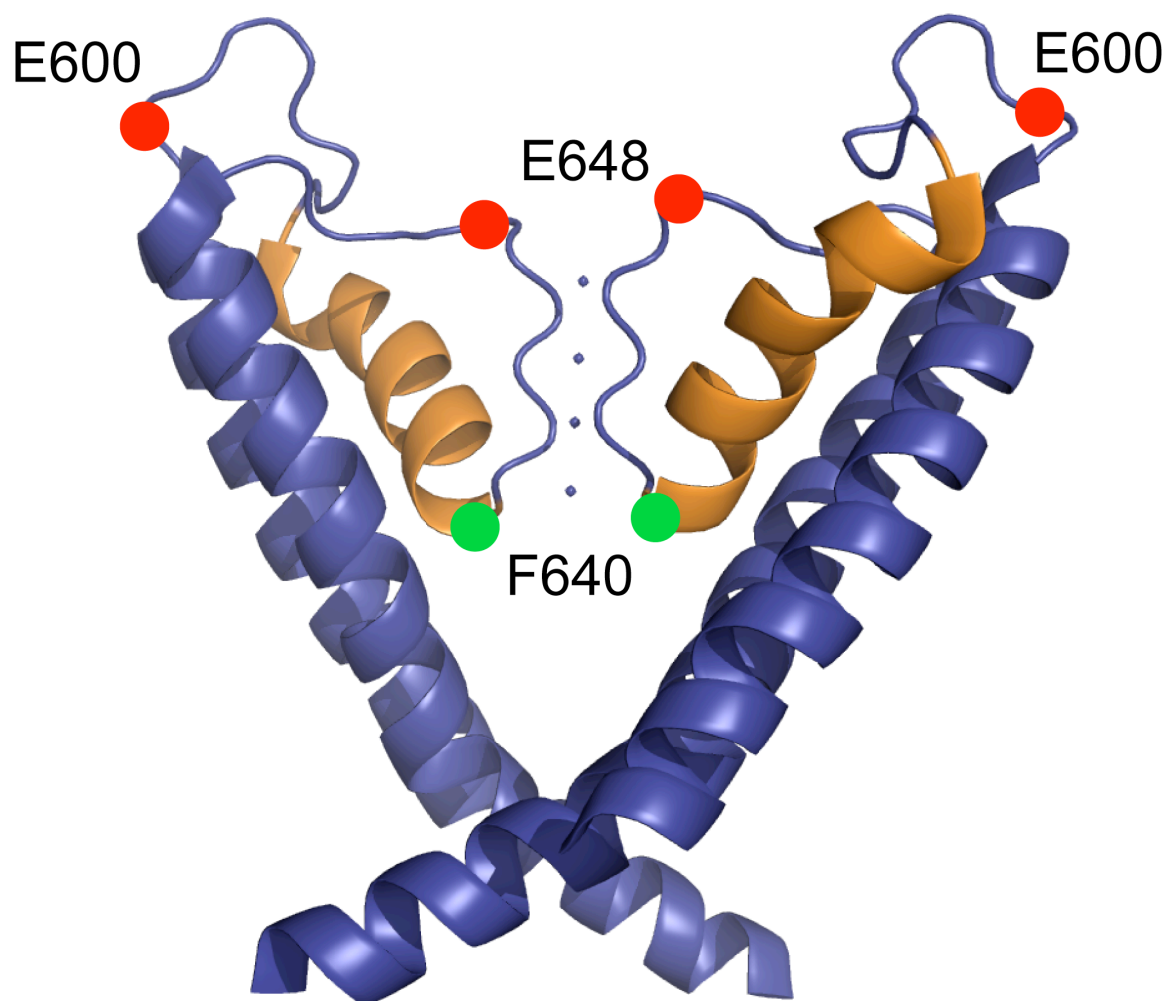


Figure 8 A structural model for the pore region of TRP channels

A model of the S5-pore-S6 region of TRPV1 as inspired by the Kv1.2 structure (PDB: 2R9R), prepared with PyMOL software (Delano, 2002). The pore helix is shown in orange. Relative location of the F640 residue is shown in green, and E600 and E648 residues previously implicated in proton modulation are shown in red.

Figure 9

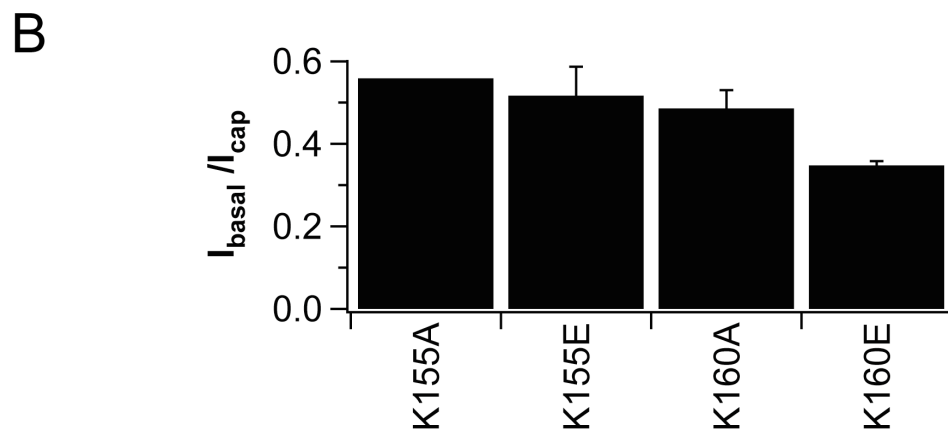
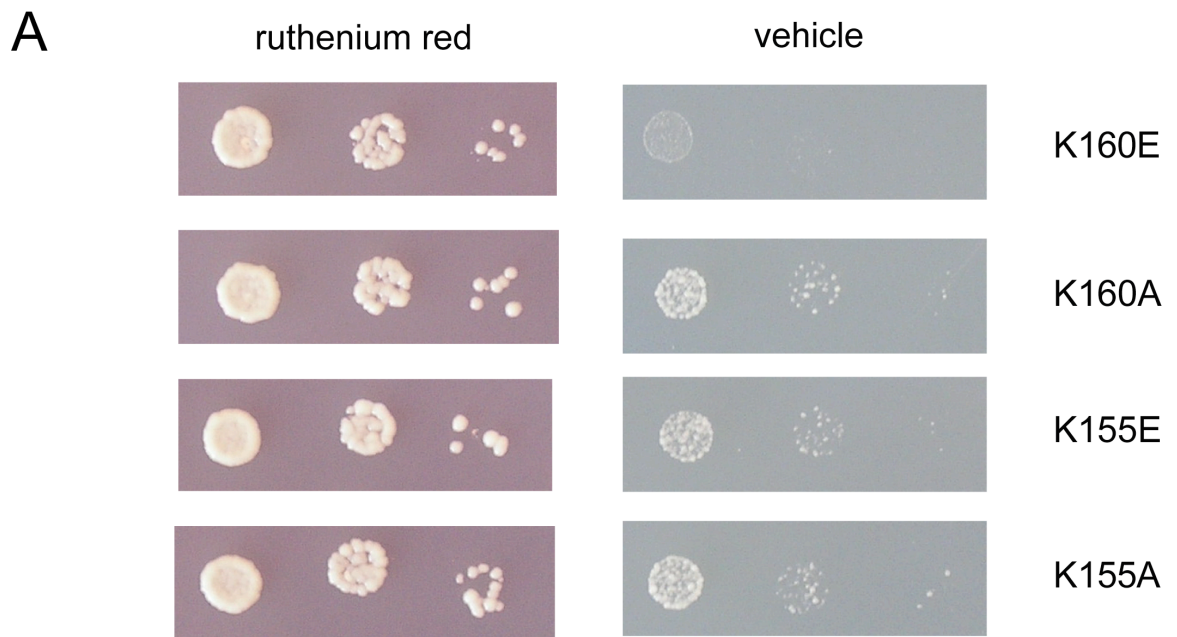
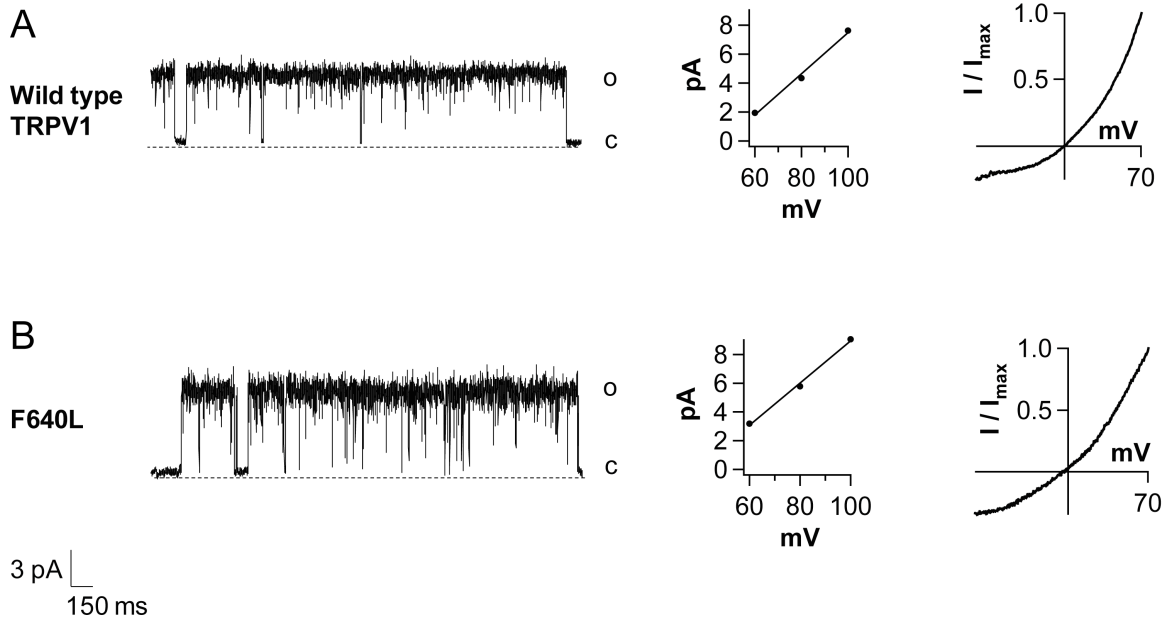


Figure 9 Mutations recovered in the TRPV1 N-terminus affect channel activation

(A) Yeast growth assay and **(B)** TEVC analysis of basal currents for alanine or glutamate substitutions of N-terminal K155 and K160 residues. Yeast growth assays and electrophysiological experiments were performed as outlined in figures 1 and 3, respectively.

Figure 10



C

Channel	P_K / P_{Na}	P_{Ca} / P_{Na}
wild type TRPV1	1.22 ± 0.08	4.89 ± 2.25
F640L	1.13 ± 0.12	6.28 ± 0.80

Figure 10 The F640L mutation does not affect TRPV1 single channel conductance or ion permeation properties

Single-channel currents were recorded in the cell-attached configuration from HEK293 cells transfected with wild type TRPV1 (**A**) or the F640L mutant (**B**). The pipette solution contained 1 μ M capsaicin. Recording were performed at pipette potentials of +60 to +100 mV and the slope conductance was calculated by linear regression, yielding values of 155.3 ± 8.1 pS vs. 147.0 ± 5.6 pS for wild type and F640L, respectively (n = 3). Single channel i-V relations were determined by ensemble averaging of leak-subtracted voltage ramp traces from excised inside-out patches and normalized to the maximal current at +70 mV. The pipette solution contained 1 μ M capsaicin. (**C**) Relative ion permeability ratios of capsaicin-evoked currents from wild type or F640L mutant channels were estimated from reversal potential shifts in whole cell patch clamp recordings of transfected HEK293 cells, revealing no significant differences.

Table 1. Summary of Yeast Screens of Mutant Libraries.

Mutant Library	Library Complexity	Average # of Amino Acid Mutations Per Clone	# of Clones Screened	# Scored as Gain-of-function	Hit Rate
N-terminus	6.8×10^4	1.67	1.3×10^4	20	0.15%
C-terminus	1.8×10^5	1.67	3.3×10^4	26	0.08%
Pore Helix	1.5×10^4	1.14	1.5×10^4	26	0.17%

Table 2. Summary of yeast toxicity and electrophysiological properties of TRPV1 mutants recovered from the genetic screen.

cDNA	# of Times Recovered	Yeast Toxicity	$I_{\text{basal}} / I_{\text{cap}}$	$I_{\text{pH 6.4}} / I_{\text{cap}}$	Constitutive Activity? _{1,2}	Potentiation? ²
C73S	1	strong	0.080 ± 0.003	0.007 ± 0.003		
I75F	1	weak	-0.010 ± 0.034	0.020 ± 0.010		
I76T	1	weak	-0.060 ± 0.041	0.022 ± 0.018		
V78G	1	weak	0.000 ± 0.013	0.014 ± 0.008		
K155E	3	weak	0.320 ± 0.052	0.248 ± 0.042	YES	YES
K160E	4	strong	0.427 ± 0.033	0.423 ± 0.008	YES	YES
H166R	1	weak	0.133 ± 0.011	0.276 ± 0.015		YES
N310D	2	weak	-0.020 ± 0.031	0.024 ± 0.015		
S343G	1	weak	0.050 ± 0.033	0.008 ± 0.013		
S343R	1	strong	0.020 ± 0.026	0.025 ± 0.019		
A350T	2	strong	0.000 ± 0.022	0.018 ± 0.018		
I352N	1	weak	0.040 ± 0.090	0.136 ± 0.070		YES
I352T	1	weak	0.090 ± 0.015	0.114 ± 0.024		YES
Q560R	1	weak	0.070 ± 0.035	0.128 ± 0.035		YES
Q561R	2	strong	0.070 ± 0.022	0.025 ± 0.001		
M581T	2	strong	0.208 ± 0.021	0.270 ± 0.019	YES	YES
M609T	1	strong	0.030 ± 0.021	0.012 ± 0.012		
M609V	1	weak	-0.020 ± 0.048	0.025 ± 0.012		
F640L	1	strong	0.516 ± 0.025	0.016 ± 0.015	YES	
N652D	1	strong	0.070 ± 0.009	0.088 ± 0.027		YES
L673I*	1	strong	0.070 ± 0.022	0.011 ± 0.005		
E684G	5	strong	0.109 ± 0.002	0.115 ± 0.013		YES
E684V	4	strong	0.090 ± 0.014	0.031 ± 0.011		YES
I689V	1	weak	0.050 ± 0.014	0.006 ± 0.006		
K710R	1	strong	-0.030 ± 0.031	0.014 ± 0.007		
F742S	1	strong	0.040 ± 0.003	0.031 ± 0.014		
W787R	1	strong	-0.030 ± 0.011	0.013 ± 0.003		
L792P	1	weak	0.050 ± 0.008	0.094 ± 0.013		YES
L796P	1	strong	-0.010 ± 0.010	0.010 ± 0.011		
L796V	1	weak	0.020 ± 0.010	0.023 ± 0.012		
WT			0.000 ± 0.020	0.015 ± 0.003		

¹ Mutants showing $I_{\text{basal}}/I_{\text{cap}} \geq 15\%$ were classified as constitutively active.

² For mutants scoring positive in each category, $p \leq 0.05$ compared to wild-type TRPV1 (Student's t-test).

* For L673I, responses were normalized to 100 μM capsaicin.

ACKNOWLEDGMENTS

We thank members of the Julius lab for advice and encouragement at all stages of this project. We are especially grateful to D. Minor for valuable suggestions on establishing the yeast assays and H-h. Chuang, A. Priel, and Y. Kirichok for guidance on electrophysiological experiments. We thank H. Madhani, J. Weissman, and members of their labs for strains, plasmids, and assistance with yeast methods. We also thank R. Nicoll, D. Bautista, A. Chesler, D. Minor, and H-h. Chuang for insightful discussions and criticism of the manuscript. This work was supported by an American Heart Association Predoctoral Fellowship (B.R.M.), a UCSF Neuroscience NIH Training Grant (C.J.B.), and grants from the National Institutes of Health (NINDS) (D.J.).

CHAPTER 3.

A Cold-activated TRP Channel Ortholog from *Xenopus laevis* Displays Alterations in Responsiveness to Thermal Stimuli.

ABSTRACT

Members of the TRP family of cation channels serve as detectors of noxious heat and cold in mammalian somatosensory neurons. In mammals, members of the TRP superfamily are tuned to different temperature ranges to allow for appropriate thermoreception under a variety of environmental conditions. However, it is unclear whether receptors from animals that live in more extreme environments show corresponding alterations in their response properties. Here we show that the South African clawed frog *Xenopus laevis* expresses an ortholog of TRPM8, previously characterized as a receptor for moderate cold in mammals. Strikingly, the temperature-response profile of *Xenopus* TRPM8 is shifted toward lower temperatures compared to the rat and chicken receptors, with a positive correlation between TRPM8 response threshold and species core body temperature. Our results suggest that species-specific differences in thermosensitivity can be attributed at least in part to intrinsic biophysical properties of temperature-gated channels in peripheral sensory neurons.

INTRODUCTION

The ability to sense ambient temperature and distinguish noxious from innocuous environmental stimuli is a fundamentally critical process for all organisms. Several excitatory transient receptor potential (TRP) cation channels have been shown to play important roles as detectors of noxious chemical and thermal stimuli in mammalian somatosensory neurons (Dhaka et al., 2006; Julius, 2005; Venkatachalam and Montell, 2007). For example, mammalian TRPV1 serves as the receptor for capsaicin (the pungent ingredient in “hot” chili peppers) and noxious heat ($> 43^{\circ}\text{C}$) (Caterina et al., 1997), while TRPM8 is activated by menthol (a “cooling” chemical compound derived from the mint plant) and moderate cold ($< 26^{\circ}\text{C}$) (McKemy et al., 2002; Peier et al., 2002a). The thermal activation ranges for TRPV1 and TRPM8 correspond well to the

temperatures of mammalian ecological niches, a functional property that likely contributes to the biological utility of TRP channels as detectors of noxious heat and moderate cold under physiological conditions. Indeed, mice deficient in either TRPV1 (Caterina et al., 2000; Davis et al., 2000) or TRPM8 (Bautista et al., 2007; Colburn et al., 2007; Dhaka et al., 2007) display pronounced defects in responses to cognate pharmacological and thermal stimuli at both cellular and behavioral levels, illustrating that, in mammals, TRP channels play a physiologically relevant role in the detection of noxious chemical and thermal agents.

While several key TRP channels that regulate mammalian temperature transduction have been examined in considerable detail, less attention has been devoted to the molecular basis of thermoreception in other animals. Sequences corresponding to TRPV1 and TRPM8 can be found in genomes spanning the entire animal kingdom, including amphibians and reptiles (Saito and Shingai, 2006), suggesting that these molecules may contribute to thermosensation in nonmammalian species as well. Interestingly, many of the species that express TRP channels are cold-blooded (or poikilothermic) rather than warm-blooded (or homeothermic), such that their core body temperature is not fixed but varies directly with the ambient environmental temperature. Because the process of thermoreception involves the measurement of temperature differences between environment and nociceptor terminal, it is possible that sensory neurons from cold-blooded animals are tuned to respond optimally to temperatures near those of their own environments. In this case, alteration of TRP channel thermal activation properties across evolution would represent an efficient regulatory mechanism to ensure that sensory neurons respond only to thermal stimuli within a range appropriate to an animal's ecological niche. However, it has not been possible to test this hypothesis because, to date, TRPV1 and TRPM8 channels have only been

examined from homeothermic species that live in relatively similar environments and display only modest variations in core body temperature.

Here, we report the cloning and characterization of TRPV1 and TRPM8 from the sensory neurons of a South African clawed frog, *Xenopus laevis*. Because this poikilothermic animal lives mostly in ponds and rivers within sub-Saharan Africa, its core body temperature range (16-22°C) is substantially colder than that of mammals (Hirsch et al., 2002; Loumont, 1984). We demonstrate a striking shift in the thermal response properties of *Xenopus laevis* TRPM8 compared to its mammalian and avian counterparts, supporting the notion that, within a given species, the properties of temperature-sensitive TRP channels are under strong evolutionary pressure to conform to a physiologically relevant temperature range.

RESULTS

Identification of TRPM8 orthologs in *Xenopus*

To learn more about the conservation of temperature detection mechanisms across animal evolution, we searched for orthologs of the mammalian cold and menthol receptor TRPM8 in distantly related species, focusing our attention on poikilothermic animals residing in ecological niches differing substantially from those of mammals. We performed homology searches of numerous publicly available genome sequences using previously reported mammalian and avian TRPM8 sequences. In this manner, we identified a partial *Xenopus tropicalis* sequence that displayed 73% amino acid sequence identity to both rat and chicken TRPM8, consistent with the results of a previous bioinformatic survey (Saito and Shingai, 2006). The open reading frame we identified is predicted to be the closest sequence match to TRPM8 within the *Xenopus tropicalis* genome. We did not locate sequences corresponding to TRPM8 in any fish

genomes, suggesting that the TRPM8 gene is absent from pre-tetrapod species and is likely to have originated during the evolution of amphibians.

We used the *Xenopus tropicalis* sequence to clone a full-length TRPM8 gene from the sensory ganglia of *Xenopus laevis*, a related species of South African clawed frog whose preferred ambient temperature is significantly colder than that of *Xenopus tropicalis* or mammals (16-22°C for *laevis* vs. 25-28°C for *tropicalis* and ~37°C for mammals), via RT-PCR amplification followed by 5' and 3' RACE (Fig. 11A). *Xenopus laevis* TRPM8 displays 74% and 76% sequence identity to rat and chicken TRPM8, respectively (Fig. 12). *In situ* hybridization experiments reveal expression of the TRPM8 transcript in the cell bodies of *Xenopus laevis* dorsal root ganglion neurons (Fig. 11B). Like its mammalian and avian orthologs, *Xenopus laevis* TRPM8 is predicted to contain six transmembrane domains with intracellular N- and C-termini, as well as an intact C-terminal coiled-coil motif that likely functions in assembly and trafficking of the mature oligomeric channel complex. In the same vein, using a genome sequence predicted to correspond *Xenopus tropicalis* TRPV1 (60% identity to the rat receptor), we also cloned a full-length copy of *Xenopus laevis* TRPV1 (Fig. 13).

A previous bioinformatic study found that, while mammalian and avian genomes appear to harbor only one copy of the TRPM8 gene, the *Xenopus tropicalis* genome also contains a second, more distantly related version of TRPM8 (TRPM8-b) (Saito and Shingai, 2006). Consistent with these results, we successfully amplified a TRPM8-b cDNA from *Xenopus laevis* sensory ganglia in the course of our studies (Table 3). TRPM8-b might encode a full-length channel in *Xenopus laevis*, as assessed by the presence of six predicted transmembrane helices and a C-terminal assembly domain. However, we were unable to detect any basal- or agonist-evoked activity from TRPM8-b

heterologously expressed in frog oocytes or mammalian cells. We also failed to observe any enhancement or diminution of currents mediated by *Xenopus laevis* TRPM8 upon coexpression of TRPM8-b (data not shown). It is possible that TRPM8-b is a pseudogene, explaining its lack of observed functionality and its disappearance in post-amphibian evolution. Alternatively, TRPM8-b could form a functional channel whose cognate activating stimulus is as yet unknown.

Functional characterization of TRPM8 species orthologs reveals dramatic alterations in thermal response properties

Because of the different mode of core body temperature regulation and altered ecological niche between amphibians and rodents, we asked whether *Xenopus laevis* TRPM8 displays variations in its pharmacological and thermal responsiveness compared to the mammalian receptor. We examined the biophysical properties of *Xenopus laevis* TRPM8 heterologously expressed in *Xenopus* oocytes using voltage-clamp electrophysiology. We found that *Xenopus laevis* TRPM8 was robustly activated by cooling stimuli, and that responses to cold exhibited strong outward rectification (Fig. 14A, B), reminiscent of both mammalian and avian TRPM8 (Chuang et al., 2004; McKemy et al., 2002; Peier et al., 2002a). However, in contrast to its mammalian and avian counterparts, *Xenopus laevis* TRPM8 exhibited marginal basal activity at room temperature, requiring stimulation at temperatures below 14°C before any cold-evoked inward currents could be confidently detected (Fig. 14A, B). Comparison of the cold-evoked outward currents for multiple TRPM8 species orthologs revealed a dramatic leftward shift in the temperature-response curve of *Xenopus laevis* TRPM8 compared to its rat and chick counterparts (Fig. 14C). Indeed, *Xenopus laevis* TRPM8 exhibited substantial cold responsiveness only at temperatures where the rat and chick receptors already showed near-saturating cold activation, corresponding to a shift in half-maximal

temperature activation of greater than 17°C. Consistent with a previous report, we also found that chicken TRPM8 exhibits a slightly higher thermal activation threshold compared to the rat receptor, a phenomenon that presumably reflects the higher core body of birds compared to mammals (Chuang et al., 2004) (Fig. 14C). Intriguingly, for the three species examined here, we noted a linear correlation between a species' core body temperature and the temperature at which its TRPM8 protein is half-maximally activated by cold ($R^2 = 0.97926$; Fig. 14D). This trend suggests that the thermal activation properties of TRPM8 are altered throughout evolution to allow for efficient cold transduction at or near the temperature range of a species' cutaneous nociceptors.

Despite this dramatic difference in thermal response properties, we found that the activation of *Xenopus laevis* TRPM8 by menthol was largely similar to that of the mammalian and avian orthologs. In electrophysiological experiments, bath application of menthol produced robust activation of *Xenopus laevis* TRPM8 (Fig. 15A, D), although responses displayed reduced potency compared to those observed from cells expressing the rat receptor (Fig. 15C; EC_{50} values of $26.4 \pm 3.6 \mu\text{M}$ and $160.1 \pm 5.8 \mu\text{M}$ for rat and *Xenopus laevis* TRPM8, respectively). Because the level of basal receptor activity influences menthol activation of TRPM8 at room temperature, it is possible that this difference in potency reflects a lower level of *Xenopus laevis* TRPM8 thermal activation at room temperature rather than an intrinsic difference in receptor affinity for menthol. We also found that menthol-evoked inward currents were suppressed by a moderate rise in bath temperature (Fig. 15A), illustrating that, as observed for mammalian and avian receptors (Chuang et al., 2004; McKemy et al., 2002; Peier et al., 2002a), ligand and temperature gating processes are synergistically coupled for *Xenopus laevis* TRPM8 as well. Like mammalian TRPM8, responses of *Xenopus laevis* TRPM8 to menthol showed strong outward rectification in cell-attached membrane

patches and ran down almost immediately upon formation of the inside-out configuration (Fig. 15B), a process that has been attributed to depletion of the cellular phospholipid PIP_2 upon patch excision (Liu and Qin, 2005; Rohacs et al., 2005). Thus, we conclude that *Xenopus laevis* TRPM8 is a *bona fide* menthol receptor with properties largely reminiscent of its mammalian and avian orthologs.

Previous work has shown that, while rat TRPM8 is robustly activated by nanomolar concentrations of the synthetic super-cooling compound icilin only when extracellular Ca^{2+} is present, chicken TRPM8 is icilin-insensitive, even in the presence of extracellular Ca^{2+} (Chuang et al., 2004; McKemy et al., 2002). The structural determinant of this pharmacological difference is a single glycine-to-alanine polymorphism in the cytoplasmic linker between the second and third transmembrane domains in chicken TRPM8 (Chuang et al., 2004). We found that, like chicken TRPM8, *Xenopus laevis* TRPM8 was completely unresponsive to icilin, even when applied at 10 μM for more than ten minutes in the presence of 2 mM extracellular Ca^{2+} (Fig 15D). Examination of the *Xenopus laevis* TRPM8 amino acid sequence reveals that it possesses the same glycine-to-alanine polymorphism reported for chicken TRPM8 (Fig. 12), a sequence divergence that likely underlies its inability to undergo icilin activation. Thus, consistent with previous reports, activation by icilin appears to be a property unique to mammalian TRPM8.

In summary, we find that while *Xenopus laevis* TRPM8 exhibits pharmacological characteristics similar to those observed in the orthologous receptors from mammals and birds, its thermal sensitivity is dramatically shifted such that substantial activation only occurs at extremely cold temperatures. This property is consistent with the substantially lower core body temperature of *Xenopus laevis* compared to homeothermic

species. Together with data from rat and chicken receptors, our findings illustrate that the thermal activation properties of TRPM8 are intimately connected with the characteristics of an animal's ecological niche.

***Xenopus laevis* TRPV1 is a weakly capsaicin-sensitive channel**

We also examined the pharmacological properties of heterologously expressed *Xenopus laevis* TRPV1 using voltage clamp electrophysiology in frog oocytes. Mammalian and avian TRPV1 channels are activated by extracellular protons (pH < 6.4), a pharmacological characteristic that likely accounts for the enhanced chemical and thermal sensitivity of TRPV1 in the context of tissue injury, which often produces acidosis localized near the site of inflammation (Caterina et al., 1997; Tominaga et al., 1998). Similarly, we found that exposure of *Xenopus laevis* TRPV1-expressing oocytes to a pH 5.3 solution led to robust inward currents at room temperature (Fig. 16A). We also found that *Xenopus laevis* TRPV1 was activated by a high concentration of capsaicin (10 μ M) in both whole cell and excised inside-out patch configurations (Fig. 16A, C). However, for the *Xenopus laevis* channel the efficacy of capsaicin is clearly less than that of protons (Fig. 16A), in contrast to the maximal receptor activation observed with capsaicin stimulation of rat TRPV1 (Jordt and Julius, 2002; Premkumar et al., 2002; Tominaga et al., 1998). Also unlike the mammalian orthologs (Hu et al., 2004), we failed to observe any activation of *Xenopus laevis* TRPV1 by the broad-spectrum TRP channel agonist 2-APB (500 μ M) (Fig. 16A). Proton-evoked responses were strongly modulated by changes in bath temperature (Fig. 16B), illustrating that *Xenopus laevis* TRPV1 is activated by heat and that the thermal and chemical activation gating mechanisms are synergistically coupled for this channel, as has been observed with other TRPV1 orthologs (Jordt and Julius, 2002; Tominaga et al., 1998).

Functional expression of *Xenopus laevis* TRP channels is strongly temperature-dependent

Xenopus laevis TRPM8 gave rise to large menthol- and cold-evoked currents when heterologously expressed in *Xenopus laevis* oocytes. We were therefore surprised to find that these channels failed to produce detectable increases in intracellular Ca^{2+} upon cold or menthol stimulation when expressed in mammalian HEK293 kidney cells (Fig 17A). We were also unable to observe any spontaneous channel activity in cell-attached patches from HEK293 cells expressing *Xenopus laevis* TRPM8, even though such activity was readily detected in *Xenopus laevis* oocytes (data not shown), illustrating that our inability to detect agonist-evoked rises in intracellular Ca^{2+} in HEK293 cells was likely due to faulty channel expression, rather than a lack of channel Ca^{2+} permeability. We obtained similar results for capsaicin activation of *Xenopus laevis* TRPV1, suggesting that the inability to form functional channels in HEK293 cells under standard culture conditions may be a general property of *Xenopus laevis* TRP channels. To determine whether the observed lack of functional expression reflected an alteration in the biochemical properties of the channel protein, we examined the detergent solubility of mammalian and amphibian TRPM8 in HEK293 cells. We found that, although the functional rat TRPM8 channels partitioned almost exclusively into a detergent-soluble cellular fraction, *Xenopus laevis* TRPM8 channels were largely detergent-insoluble (Fig. 17B). Thus, the compromised functionality of *Xenopus laevis* TRP channels in mammalian cells correlates with an inability to form properly folded, detergent-soluble protein complexes.

What is the basis for the lack of functional expression in mammalian cells? One important difference between HEK293 cells and *Xenopus laevis* oocytes is the temperature at which they are incubated for routine culture (37°C for HEK293 cells vs.

16°C for *Xenopus laevis* oocytes.) Because the core body temperature of *Xenopus laevis* is typically at least 15°C less than that of mammals, we suspected that the standard incubation temperature for mammalian cells might render *Xenopus laevis* TRP channels biochemically unstable, leading to detergent insolubility and defective functionality in transfected HEK293 cells. We therefore asked whether a transient reduction in incubation temperature for *Xenopus laevis* TRPM8-expressing HEK293 cells could rescue functional channel expression. Indeed, when TRPM8-expressing HEK293 cells were incubated at 30°C for six hours prior to ratiometric Ca²⁺ imaging experiments, we were able to observe clear, robust rises in intracellular Ca²⁺ upon menthol stimulation (Fig. 17A). We found a similar dependence on HEK293 cell incubation temperature for capsaicin activation of *Xenopus laevis* TRPV1, as assessed by ratiometric Ca²⁺ imaging. We also found that the *Spodoptera frugiperda* Sf9 insect cell line, routinely incubated at 27°C, supported the functional expression of *Xenopus laevis* TRPV1 and TRPM8 in Ca²⁺ imaging experiments (data not shown). Thus, the inability of *Xenopus laevis* TRPV1 and TRPM8 to function in HEK293 cells under standard culture conditions is caused by the nonpermissive mammalian cell incubation temperature, which is inhospitable to the proper folding and expression of these channels.

DISCUSSION

In this study, we report the cloning and characterization of temperature-sensitive TRP channel orthologs from *Xenopus laevis*, a cold-blooded aquatic frog whose optimal environmental temperature is substantially lower than that of mammals (Hirsch et al, 2002; Loumont, 1984). We found that *Xenopus laevis* TRPM8 responds strongly to the plant-derived cooling compound menthol and (like its avian counterpart) is insensitive to the synthetic compound icilin, raising the possibility that icilin mimics a small molecule

TRPM8 modulator endogenous to mammals but absent in amphibians and birds. However, in comparing the thermal activation properties of several TRPM8 orthologs, we found a dramatic shift in the range of temperatures at which *Xenopus laevis* TRPM8 is gated, such that significant activation occurs only at temperatures much colder than for rat or chicken TRPM8. This shift in thermal activation corresponds well with the reduction in core body temperature (and, by extension, the temperature at the nociceptor terminal) that would be expected in this poikilothermic species. Indeed, for the three TRPM8 species orthologs examined in this study (rat, chicken, and *Xenopus laevis*) we found a striking correlation between the species' core body temperature and the temperature required to observe half-maximal TRPM8 activation, suggesting that the biophysical properties of TRPM8 in each species are tuned to the most appropriate temperature range. In the future, it will be worthwhile to examine TRPM8 orthologs from a wide range of poikilothermic and homeothermic animals, including amphibians and reptiles, to assess the extent to which species core body temperature and TRPM8 activation properties are correlated throughout evolution.

We also identified a *Xenopus laevis* ortholog of TRPV1, shown in mammals to serve as a receptor for capsaicin, protons, and noxious heat. We found that *Xenopus laevis* TRPV1 is gated by capsaicin and protons, and that proton-evoked currents are modulated by changes in ambient temperature. Although chicken TRPV1 is completely capsaicin-insensitive (Jordt and Julius, 2002), the modest capsaicin sensitivity of *Xenopus laevis* TRPV1 illustrates that TRPV1 capsaicin sensitivity is not limited to mammals, but is observed in at least some other species as well. It will be of interest to determine the precise heat activation threshold for *Xenopus laevis* TRPV1 to assess whether TRPV1 thermal gating is under evolutionary constraints as we have observed for TRPM8.

We found that heterologous expression of *Xenopus laevis* TRPM8 and TRPV1 in HEK293 cells leads to detergent insolubility and compromised functionality, but that the functional defects can be rescued by lowering the cellular incubation temperature prior to electrophysiological or Ca²⁺ imaging analysis. Such temperature-dependent defects in expression are not universally observed when receptors from *Xenopus laevis* are expressed in mammalian cells, suggesting that *Xenopus* proteins are not grossly incompatible with mammalian expression systems. For example, *Xenopus* muscarinic receptors (Herrera et al., 1997), as well as voltage-gated channels (Fry et al., 2004), retain their functionality upon heterologous expression in mammalian cells. However, a strong temperature-dependence of functionality is sometimes diagnostic of improperly folded or otherwise unstable mammalian proteins. Indeed, for loss-of-function mutants of CFTR (Denning et al., 1992) and G α -s (Iiri et al., 1994) that lead to misfolding and eventual pathogenesis, a decrease in temperature was found to permit the mutant proteins to accumulate in properly folded form and subsequently regain their wild-type functionality. We observed that, unlike the functional rat ortholog, *Xenopus laevis* TRPM8 accumulates in a detergent-insoluble fraction when heterologously expressed in HEK293 cells, suggesting that the channel may be improperly folded in this expression system under standard incubation conditions. In this regard, it will be interesting to determine whether the same prolonged low-temperature incubation that rescues *Xenopus laevis* TRPM8 functionality also leads to the acquisition of detergent solubility.

Several previous studies have demonstrated that orthologs of sensory neuronal TRP channels vary in their capacity to respond to pharmacological agonists depending on the ecological niche of the species in question. For example, the well-known insensitivity of birds to capsaicin, a feature that endows birds with the ability to act as efficient *capsicum*

seed dispersal vehicles, is manifest in chicken TRPV1 as a loss of capsaicin sensitivity (Jordt and Julius, 2002). Similarly, the icilin insensitivity observed with TRPM8 from chickens may reflect the absence of a small molecule TRPM8 modulator expressed exclusively in the mammalian sensory neuronal milieu (Chuang et al., 2004). Our study clearly demonstrates that the thermal activation properties of cold transduction channels are also sensitive to ecological and evolutionary pressure, providing an efficient mechanism by which responsiveness to different environmental niches can be altered to allow for optimal transduction of sensory information within an ideal temperature range.

EXPERIMENTAL PROCEDURES

Molecular biology

The ENSEMBL database was searched for orthologs of mammalian TRPV1 and TRPM8 channels using the previously described *rattus norvegicus* and *gallus gallus* sequences. Putative TRPV1 and TRPM8 orthologs were identified from *Xenopus tropicalis*, and internal PCR primers were designed to amplify conserved regions within each gene. Trigeminal and dorsal root neurons were dissected from adult female *Xenopus laevis* and total RNA was extracted from polytron-homogenized ganglia using TRIZOL (Invitrogen). Total RNA was reverse transcribed using SuperScript II MMLV-RT (Invitrogen), and resulting first strand cDNA was amplified using Advantage 2 polymerase (Clontech). The sequences of internal PCR products were used to obtain complete transcript sequences using 5' and 3' SmartRACE (Clontech.) Full-length genes were amplified using a high fidelity polymerase (Phusion) and captured by TA-cloning. For TRPV1, primer pairs were: 5'-GATTCAACAAAATGAAGAAAAT-3' and 5'-GACAGATTCACTCAGCCTTG-3'. For TRPM8, primer pairs were: 5'-CAGTGTGCTCTGGTCTTAGCTTTAC-3' and 5'-TCACTTTATCTTGCTTCTGATTTC-

3'. For mammalian cell experiments, genes were subcloned into pCDNA3 or pMO, and a hemagglutinin (HA) tag was added to the N-terminus for immunoblotting experiments. For insect cell experiments, genes were cloned into pBT3. For *in vitro* RNA transcription, channel constructs were linearized, transcribed (mMessage Machine T7 transcription kit, Ambion), and resuspended at a final concentration of 1 µg/µl. *In situ* hybridization was performed essentially as previously described (McKemy et al, 2002).

Oocyte culture and electrophysiology

Surgically extracted oocytes from *Xenopus laevis* (Nasco) were cultured and analyzed 2-14 days post-injection by TEVC as previously described (Chuang et al., 2004). For proton experiments, MES was substituted for HEPES and pH adjusted accordingly. For patch clamp analysis, both the bath and pipette solutions contained (in mM): 140 CsCl, 10 HEPES, 1 MgCl₂·6H₂O, 1 EGTA, pH 7.4. Macropatches were excised from devitellinized oocytes using pipettes with resistances of 0.3-1.0 MΩ and currents were recorded with an Axopatch 200B amplifier (Molecular Devices) using a 180 ms voltage ramp from -120 mV to +80 mV delivered once per second. Currents were recorded at 5 kHz, filtered at 2 kHz, and analyzed with pClamp 10 (Molecular Devices). Temperature ramps were generated with a custom-made Peltier device (Reid-Dan Electronics). Capsaicin, menthol, icilin, and 2-APB stocks were dissolved in DMSO and diluted into recording solution immediately prior to experiments.

Mammalian and insect cell culture and physiology

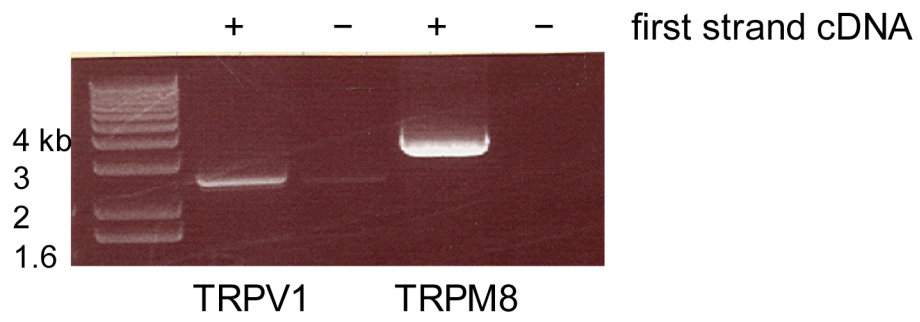
HEK293T cells were cultured and transfected as previously described (Chuang et al., 2004.) Sf9 cells were maintained in Sf900-II defined medium (Invitrogen) and transfected with Cellfectin (Invitrogen). Two days after transfection, cells were plated onto polylysine- or polyornithine-coated chamber slides, loaded for 45 minutes in Sf900-

II supplemented with 1 μ M fura2/AM and 0.02% pluronic acid, and subjected to ratiometric calcium imaging. Imaging was as previously described (Chuang et al., 2004, Bautista et al, 2007), except that MES-buffered saline (MBS) solution (in mM: 10 CaCl₂, 60 KCl, 17 MgCl₂, 10 NaCl, 4 glucose, 110 sucrose, 10 MES, 0.1% BSA, pH 6.2) was used in place of normal mammalian Ringer's solution.

Detergent extraction and immunoblotting

Two days after transfection, HEK293 cells expressing HA-tagged TRPM8 channels were lysed by trituration in standard phosphate-buffered saline supplemented with 1% Triton X-100. Lysates were clarified at 10,000 x g for 12 minutes at 4°C and supernatants were mixed with sample buffer and separated on a 7.5% SDS-PAGE gel. Cell pellets containing Triton-insoluble material were mixed with sample buffer, disrupted via sonication, and loaded onto SDS-PAGE gels. Following electrophoresis, samples were transferred to Immobilon membranes (Millipore) and blocked overnight at 4°C in PBS + 0.5% Tween-20 (PBS-T) + 3% BSA. Membranes were incubated with mouse anti-HA primary antibody (Covance, 1:4000 dilution) for 1.5 hours at room temperature, washed, incubated with HRP-conjugated goat anti-mouse secondary antibody (Jackson Research, 1:5000 dilution) for 1 hour at room temperature, and photographically developed.

A



B

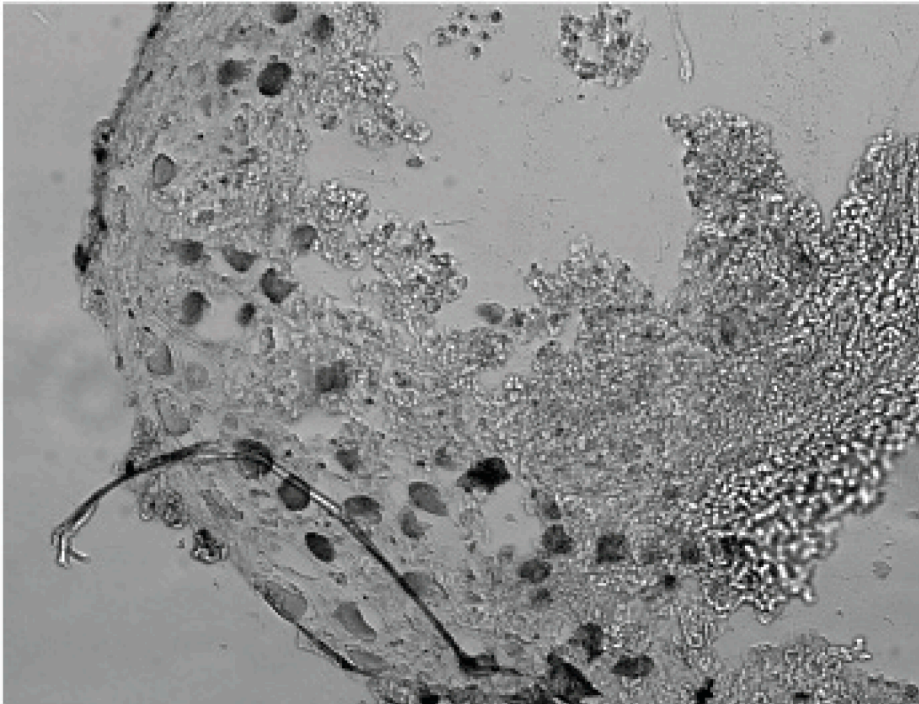


Figure 11 **Expression of TRPV1 and TRPM8 in sensory ganglia from *Xenopus laevis***

(A) RT-PCR amplification of full-length TRPV1 and TRPM8 orthologs using first strand cDNA derived from extracts of adult *Xenopus laevis* trigeminal and dorsal root ganglion neurons. Primer pairs are described in “experimental procedures” section. Lanes without first strand cDNA are shown as negative controls. **(B)** *In situ* hybridization (conducted by Yari Sigal) using an antisense riboprobe derived from *Xenopus laevis* TRPM8, performed on histological sections from adult *Xenopus laevis* dorsal root ganglia.

Figure 12

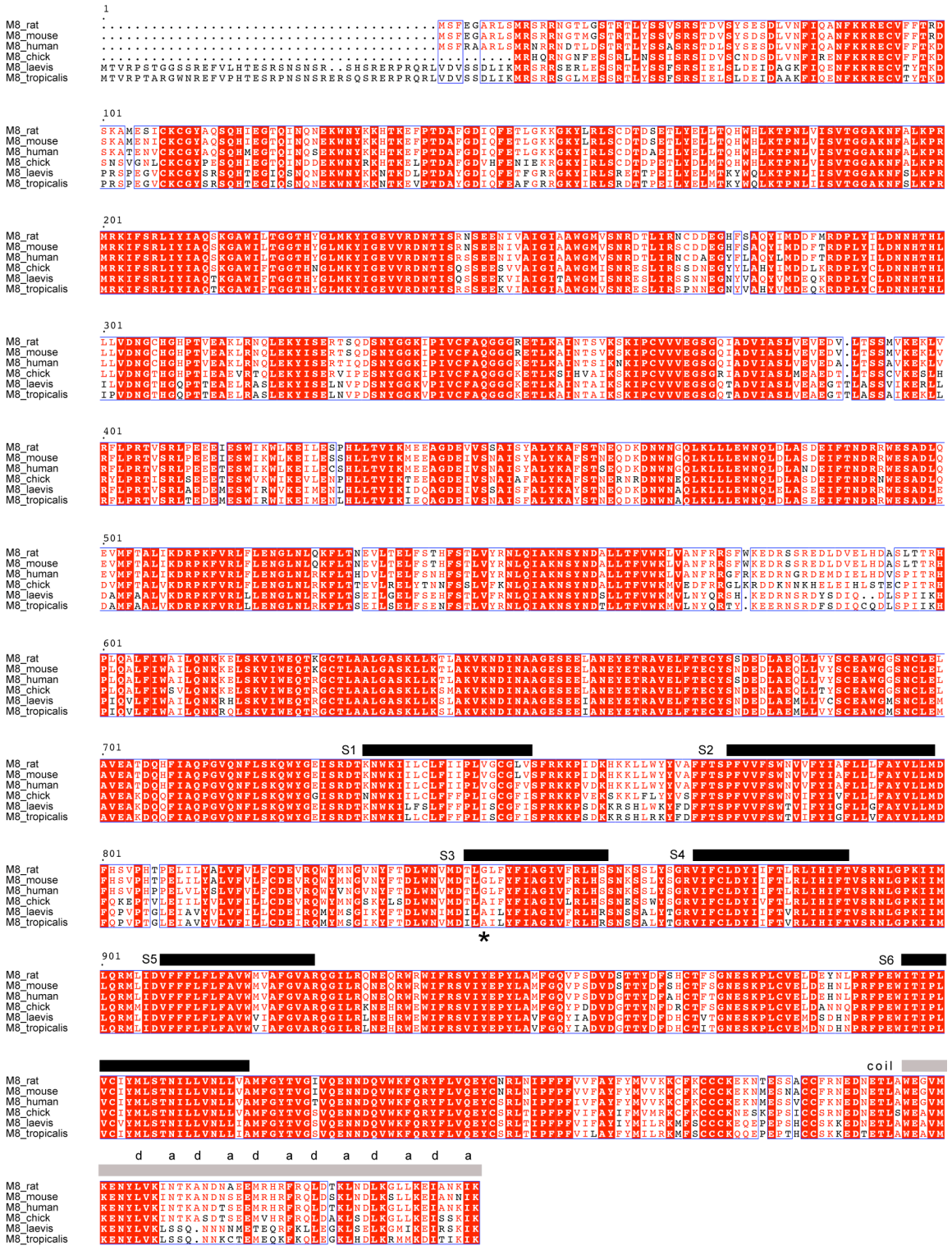


Figure 12 Sequence alignment of TRPM8 species orthologs

Previously described rat, human, and chicken TRPM8 sequences were aligned with the full-length sequences of *Xenopus tropicalis* and *Xenopus laevis* TRPM8 (this study) using MultAlin (<http://bioinfo.genotoul.fr/multalin/multalin.html>) and ESPript (<http://esprict.ibcp.fr/ESPript/ESPript/index.php>) software packages. In the alignment, red type indicates conserved residues, black type indicates neutral residues, and blue type indicates divergent residues. The locations of predicted transmembrane helices (from McKemy et al, 2002) and the C-terminal coiled-coiled assembly domain (from Tsuruda et al, 2006) are shown as black and gray bars, respectively. Within the coiled coil motif, the “a” and “d” positions are indicated for each heptad repeat. The asterisk indicates the polymorphic residue which was previously shown to determine TRPM8 icilin sensitivity (Chuang et al, 2004).

Figure 13

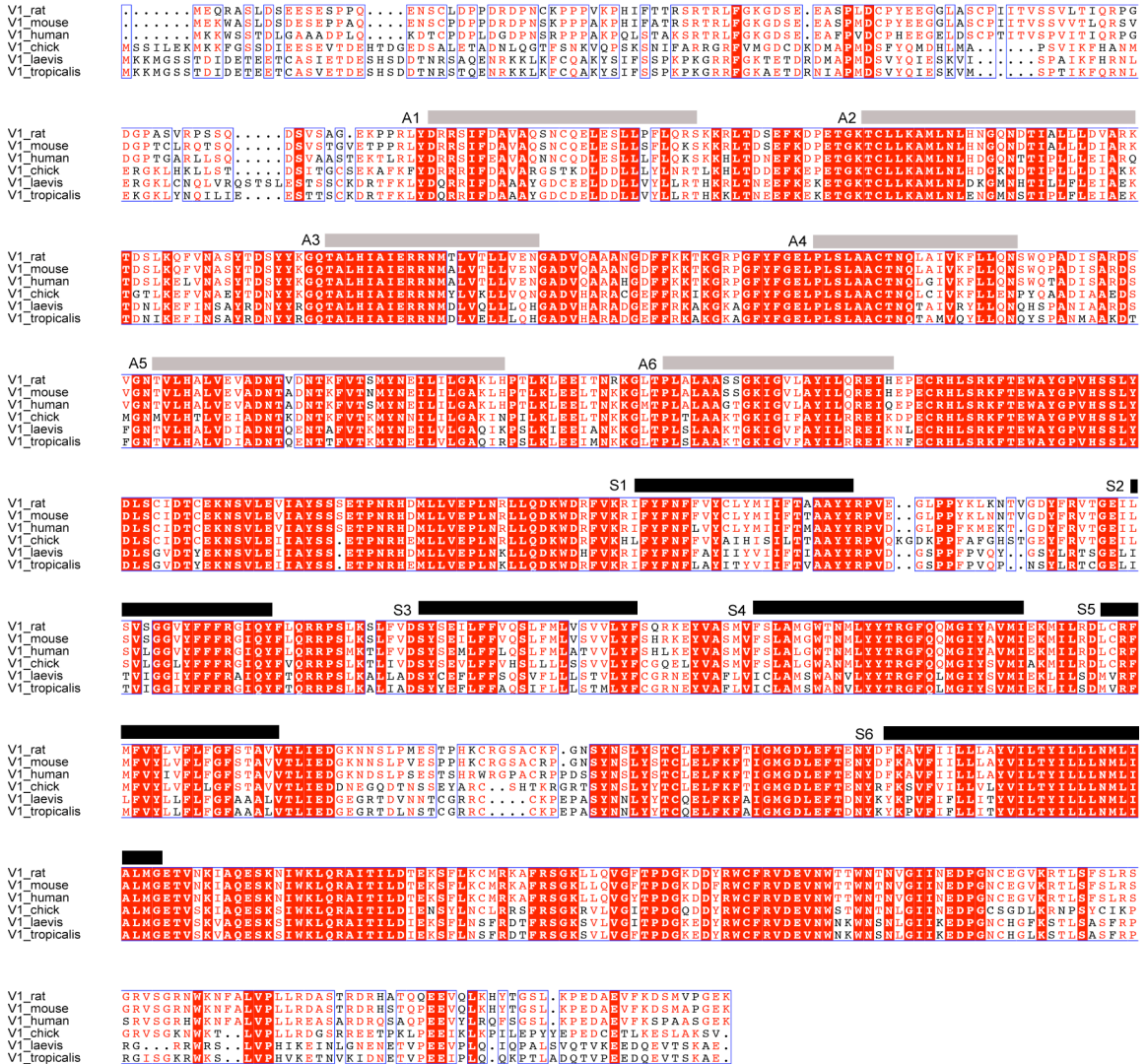


Figure 13 Sequence alignment of TRPV1 species orthologs

Previously described rat, human, and chicken TRPV1 sequences were aligned with the sequence of *Xenopus laevis* TRPV1 (this study) as in figure 12. The locations of predicted transmembrane helices (from Caterina et al, 1997) are shown as black bars, and the locations of N-terminal ankyrin repeats (from Lishko et al, 2007) are shown as gray bars.

Figure 14

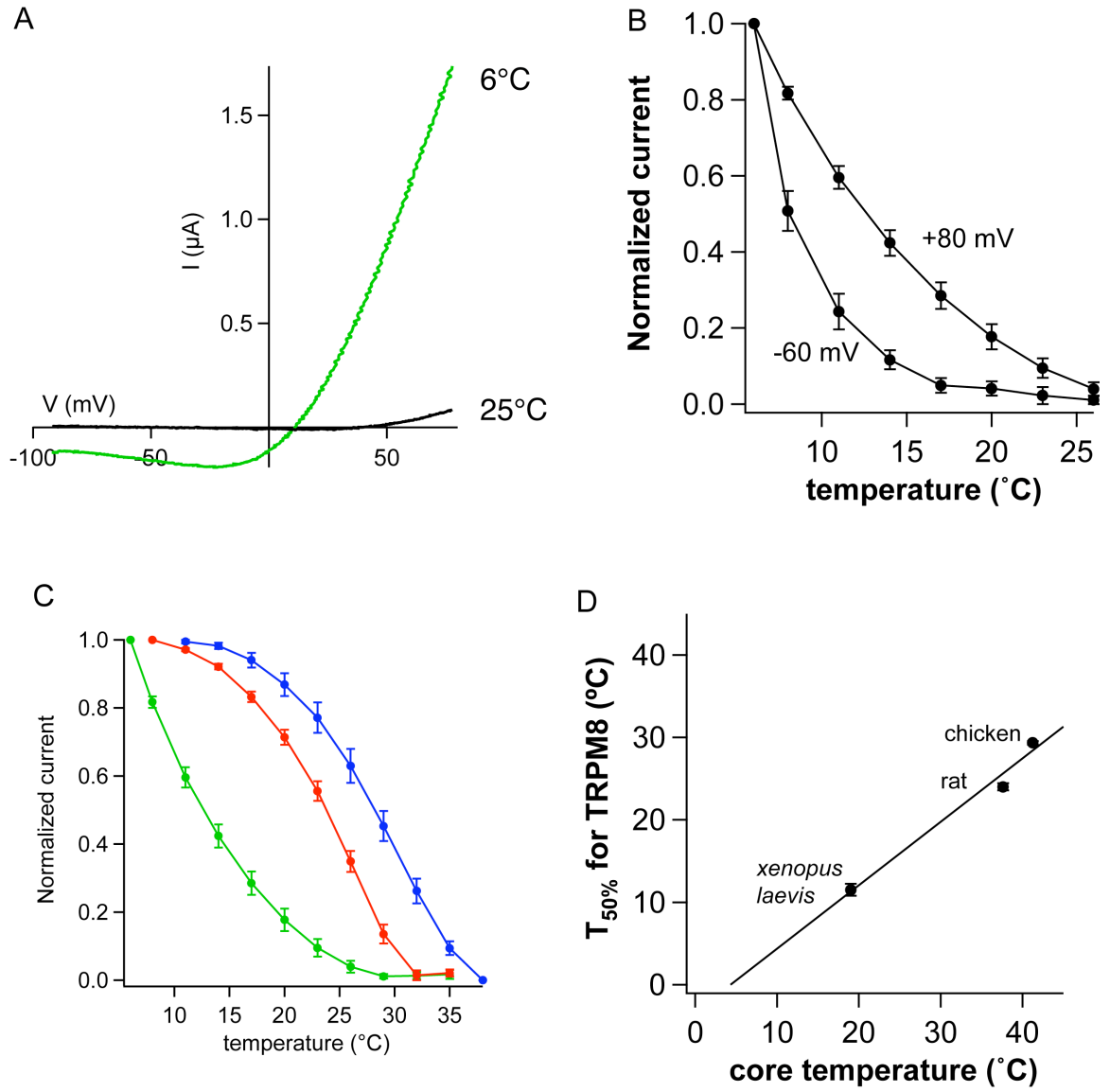


Figure 14 *Xenopus laevis* TRPM8 displays altered cold activation properties

(A) Current-voltage relation from a two-electrode voltage clamp recording of *Xenopus laevis* TRPM8-expressing oocytes under basal or cold-stimulated conditions. Note the strong outward rectification of the cold-evoked current. **(B)** Normalized inward (-60 mV) and outward (+80 mV) cold-evoked currents for *Xenopus laevis* TRPM8. For each potential, the current obtained at a given temperature was normalized to the maximum cold-evoked current (obtained at 6° C) obtained at that potential. **(C)** Normalized current-temperature plots (at +80 mV) for chicken (blue), rat (red), and *Xenopus laevis* TRPM8 (green), yielding half-maximal activation temperatures of $29.35 \pm 0.21^{\circ}\text{C}$ (chicken), $24.00 \pm 0.43^{\circ}\text{C}$ (rat), and $11.51 \pm 0.73^{\circ}\text{C}$ (*Xenopus laevis*). Note that for *Xenopus laevis* TRPM8, the accuracy of this value is limited by our inability to observe saturation of the current-temperature plot, even at the coldest temperature tested. **(D)** Plot of species core body temperature (obtained from previously published measurements) versus experimentally determined temperature of half-maximal TRPM8 cold activation reveals a linear correlation ($R^2 = 0.97926$) between these two parameters. For chicken, core temperature was obtained from (Lin et al., 2005). For rat, core temperature was obtained from (Yochim and Spencer, 1976). For *Xenopus laevis*, core temperature was estimated as the arithmetic mean from (Hirsch et al., 2002).

Figure 15

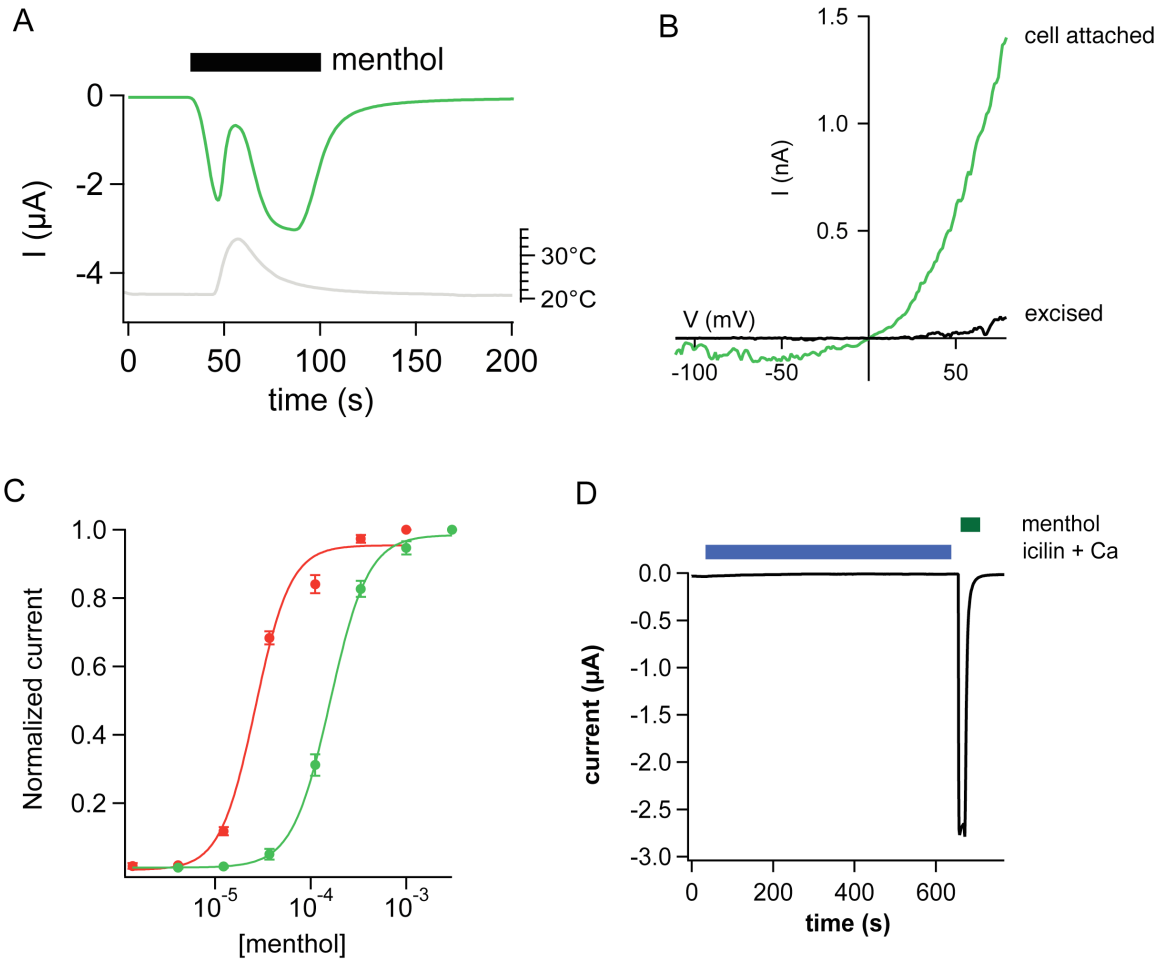


Figure 15 *Xenopus laevis* TRPM8 is activated by menthol but not icilin

(A) In oocytes expressing *Xenopus laevis* TRPM8, application of menthol (1 mM) evoked inward currents (green trace) that were suppressed by a rise in bath temperature (gray trace). Holding potential was -60 mV. **(B)** Cell-attached patches from oocytes expressing *Xenopus laevis* TRPM8 (n=4) but not uninjected oocytes (n=3) displayed a strongly rectifying current (green trace) when the pipette contained 500 μ M menthol. Formation of the inside-out configuration resulted in rapid current rundown (black trace, 90 seconds after patch excision.) **(C)** Concentration-response relation for menthol-evoked currents (at +80 mV) from rat (red) or *Xenopus laevis* (green) TRPM8-expressing oocytes. **(D)** Application of 10 μ M icilin in the presence of 2 mM extracellular Ca^{2+} failed to activate *Xenopus laevis* TRPM8, while 1 mM menthol evoked robust inward currents.

Figure 16

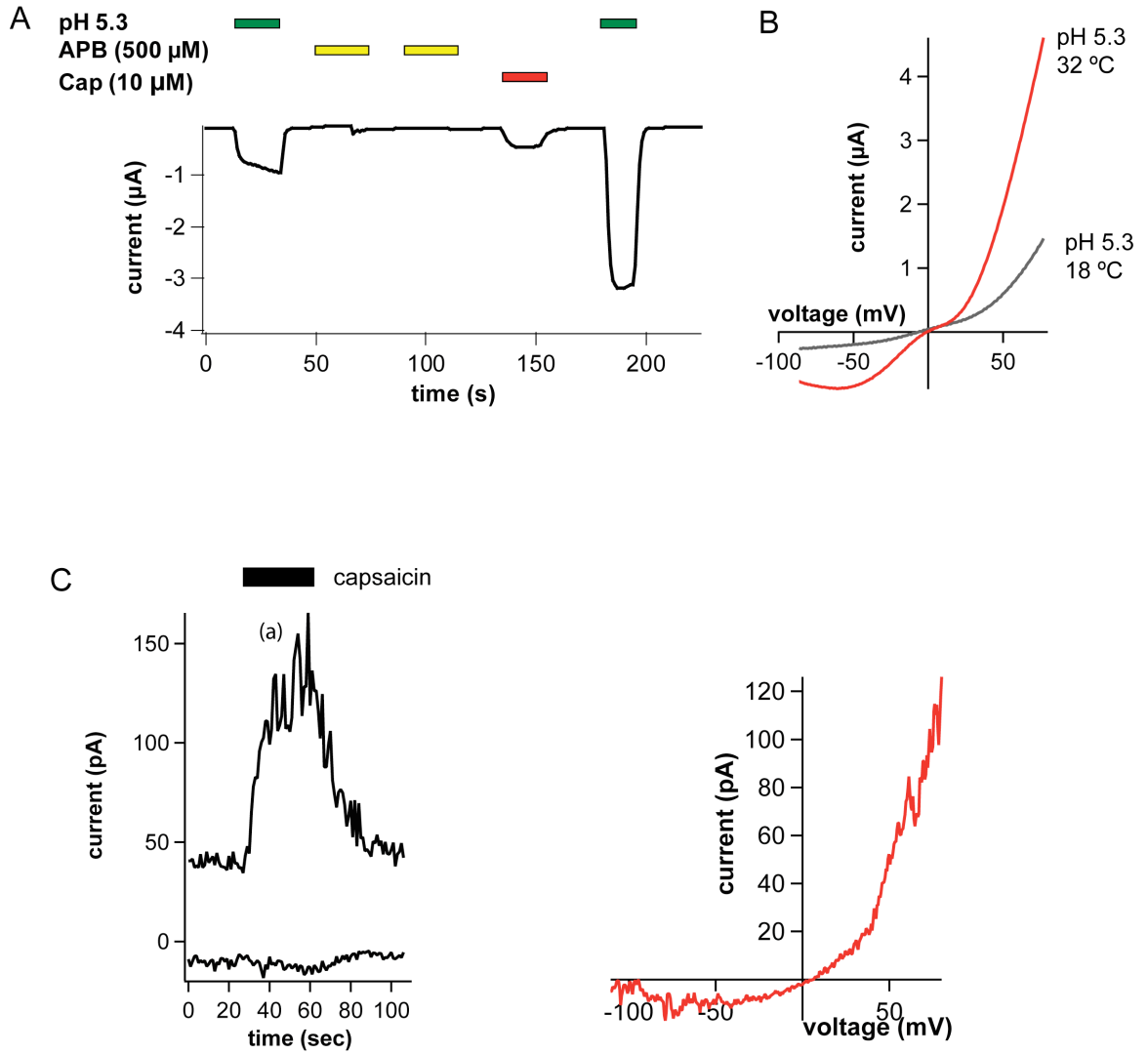


Figure 16 *Xenopus laevis* TRPV1 is activated by protons and is weakly sensitive to capsaicin.

(A) Inward currents in oocytes expressing *Xenopus laevis* TRPV1 and exposed to protons, capsaicin, or 2-APB at the indicated concentrations. **(B)** Current-voltage relation from two-electrode voltage clamp recording performed on *Xenopus laevis* TRPV1-expressing oocytes. For the proton-evoked current, a rise in bath temperature from 18°C (black) to 32°C (red) resulted in dramatic current potentiation. **(C)** Application of 10 μ M capsaicin to an excised patch from *Xenopus laevis* TRPV1-expressing oocytes yielded a strongly outwardly rectifying current. Both inward and outward currents (at -60 mV and +80 mV, respectively) are shown. Graph at right shows the leak-subtracted current-voltage relation at point “a” in the graph at left.

Figure 17

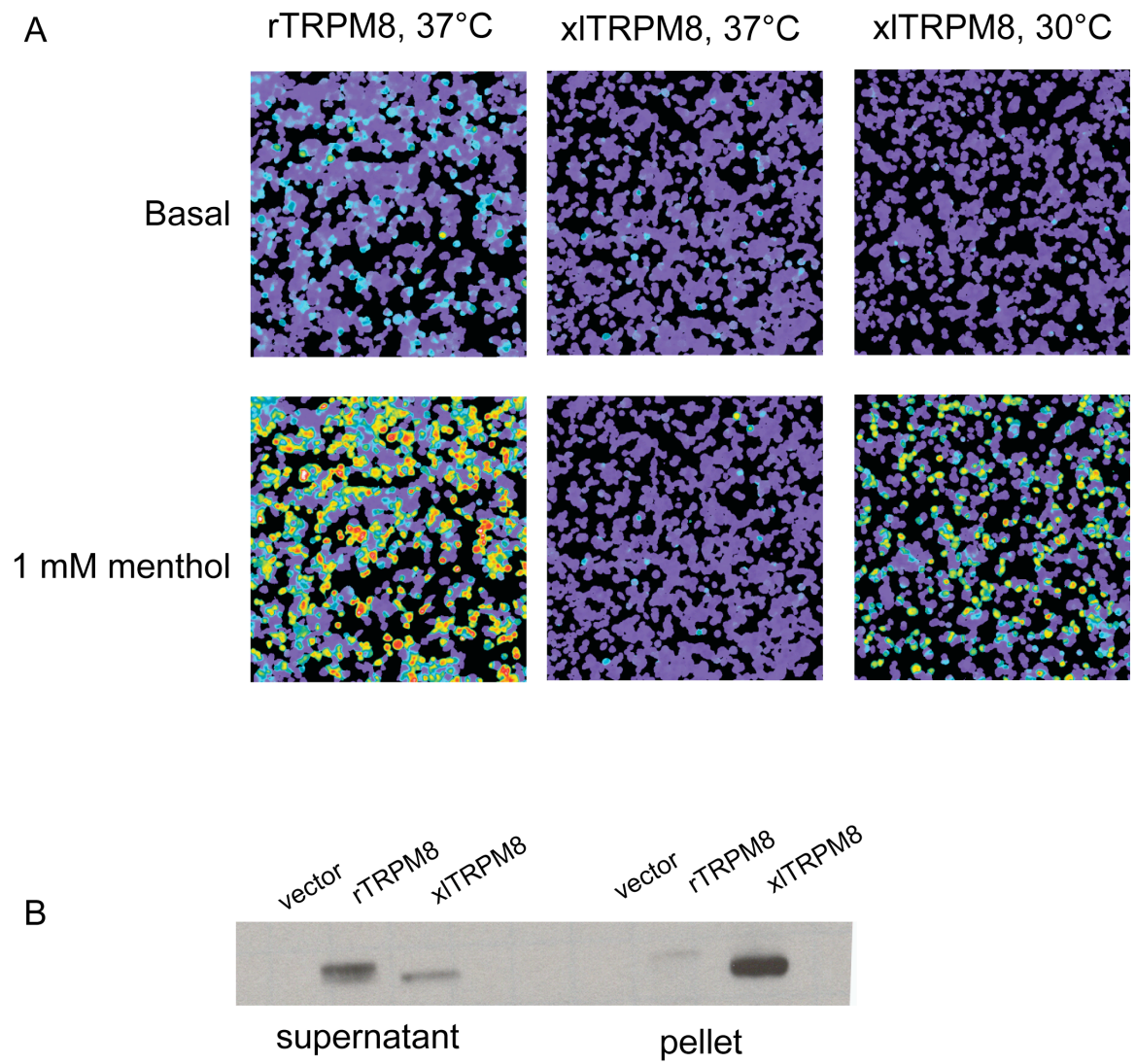


Figure 17 Functional expression of *Xenopus laevis* TRPM8 is temperature-dependent

(A) Ratiometric fura2 Ca^{2+} imaging of HEK293 cells transfected with rat or *Xenopus laevis* TRPM8. On the day of the experiment, cells were incubated at either 37 or 30°C for six hours prior to imaging. Cells were imaged either in the presence or absence of 1 mM menthol. **(B)** Immunoblot analysis of HEK293 cells transfected with HA-tagged rat or *Xenopus laevis* TRPM8 genes or a vector control after solubilization in lysis buffer containing Triton X-100 as described in “experimental procedures.” Samples represent either the supernatant (soluble) or pellet (insoluble) after Triton extraction.

Table 3. Percent amino acid similarity between TRPM8 species orthologs

<i>Species</i>	Rat	Chick	Laevis	Laevis b	Trop
Rat					
Chick	80				
Laevis	74	76			
Laevis b	65	65	73		
Trop	75	76	94	72	
Trop b	64	65	73	87	72

Laevis = *Xenopus laevis*; Trop = *Xenopus tropicalis*. “b” refers to the TRPM8-b gene apparently present in the *laevis* and *tropicalis* genomes.

CHAPTER 4.

Bibliography

Ahern, C.A., Eastwood, A.L., Lester, H.A., Dougherty, D.A., and Horn, R. (2006). A cation- π interaction between extracellular TEA and an aromatic residue in potassium channels. *The Journal of general physiology* 128, 649-657.

Alagem, N., Yesylevskyy, S., and Reuveny, E. (2003). The pore helix is involved in stabilizing the open state of inwardly rectifying K⁺ channels. *Biophysical journal* 85, 300-312.

Asakawa, M., Yoshioka, T., Matsutani, T., Hikita, I., Suzuki, M., Oshima, I., Tsukahara, K., Arimura, A., Horikawa, T., Hirasawa, T., and Sakata, T. (2006). Association of a mutation in TRPV3 with defective hair growth in rodents. *The Journal of investigative dermatology* 126, 2664-2672.

Bandell, M., Dubin, A.E., Petrus, M.J., Orth, A., Mathur, J., Hwang, S.W., and Patapoutian, A. (2006). High-throughput random mutagenesis screen reveals TRPM8 residues specifically required for activation by menthol. *Nature neuroscience* 9, 493-500.

Bautista, D.M., Jordt, S.E., Nikai, T., Tsuruda, P.R., Read, A.J., Poblete, J., Yamoah, E.N., Basbaum, A.I., and Julius, D. (2006). TRPA1 mediates the inflammatory actions of environmental irritants and proalgesic agents. *Cell* 124, 1269-1282.

Bautista, D.M., Siemens, J., Glazer, J.M., Tsuruda, P.R., Basbaum, A.I., Stucky, C.L., Jordt, S.E., and Julius, D. (2007). The menthol receptor TRPM8 is the principal detector of environmental cold. *Nature* 448, 204-208.

Brauchi, S., Orta, G., Salazar, M., Rosenmann, E., and Latorre, R. (2006). A hot-sensing cold receptor: C-terminal domain determines thermosensation in transient receptor potential channels. *J Neurosci* 26, 4835-4840.

Caterina, M.J., Leffler, A., Malmberg, A.B., Martin, W.J., Trafton, J., Petersen-Zeitz, K.R., Koltzenburg, M., Basbaum, A.I., and Julius, D. (2000). Impaired nociception and pain sensation in mice lacking the capsaicin receptor. *Science (New York, N.Y)* 288, 306-313.

Caterina, M.J., Schumacher, M.A., Tominaga, M., Rosen, T.A., Levine, J.D., and Julius, D. (1997). The capsaicin receptor: a heat-activated ion channel in the pain pathway. *Nature* 389, 816-824.

Chatelain, F.C., Alagem, N., Xu, Q., Pancaroglu, R., Reuveny, E., and Minor, D.L., Jr. (2005). The pore helix dipole has a minor role in inward rectifier channel function. *Neuron* 47, 833-843.

Chuang, H.H., Neuhausser, W.M., and Julius, D. (2004). The super-cooling agent icilin reveals a mechanism of coincidence detection by a temperature-sensitive TRP channel. *Neuron* 43, 859-869.

Chuang, H.H., Prescott, E.D., Kong, H., Shields, S., Jordt, S.E., Basbaum, A.I., Chao, M.V., and Julius, D. (2001). Bradykinin and nerve growth factor release the capsaicin receptor from PtdIns(4,5)P₂-mediated inhibition. *Nature* 411, 957-962.

Chung, M.K., Lee, H., Mizuno, A., Suzuki, M., and Caterina, M.J. (2004a). 2-aminoethoxydiphenyl borate activates and sensitizes the heat-gated ion channel TRPV3. *J Neurosci* 24, 5177-5182.

Chung, M.K., Lee, H., Mizuno, A., Suzuki, M., and Caterina, M.J. (2004b). TRPV3 and TRPV4 mediate warmth-evoked currents in primary mouse keratinocytes. *The Journal of biological chemistry* 279, 21569-21575.

Clapham, D.E. (2003). TRP channels as cellular sensors. *Nature* 426, 517-524.

Colburn, R.W., Lubin, M.L., Stone, D.J., Jr., Wang, Y., Lawrence, D., D'Andrea, M.R., Brandt, M.R., Liu, Y., Flores, C.M., and Qin, N. (2007). Attenuated cold sensitivity in TRPM8 null mice. *Neuron* 54, 379-386.

Cordero-Morales, J.F., Cuello, L.G., Zhao, Y., Jogini, V., Cortes, D.M., Roux, B., and Perozo, E. (2006). Molecular determinants of gating at the potassium-channel selectivity filter. *Nature structural & molecular biology* 13, 311-318.

Davis, J.B., Gray, J., Gunthorpe, M.J., Hatcher, J.P., Davey, P.T., Overend, P., Harries, M.H., Latcham, J., Clapham, C., Atkinson, K., *et al.* (2000). Vanilloid receptor-1 is essential for inflammatory thermal hyperalgesia. *Nature* *405*, 183-187.

Decailot, F.M., Befort, K., Filliol, D., Yue, S., Walker, P., and Kieffer, B.L. (2003). Opioid receptor random mutagenesis reveals a mechanism for G protein-coupled receptor activation. *Nature structural biology* *10*, 629-636.

Delano, W.D. (2002). The PyMOL Molecular Graphics System.

Denning, G.M., Anderson, M.P., Amara, J.F., Marshall, J., Smith, A.E., and Welsh, M.J. (1992). Processing of mutant cystic fibrosis transmembrane conductance regulator is temperature-sensitive. *Nature* *358*, 761-764.

Dhaka, A., Murray, A.N., Mathur, J., Earley, T.J., Petrus, M.J., and Patapoutian, A. (2007). TRPM8 is required for cold sensation in mice. *Neuron* *54*, 371-378.

Dhaka, A., Viswanath, V., and Patapoutian, A. (2006). Trp ion channels and temperature sensation. *Annual review of neuroscience* *29*, 135-161.

Doyle, D.A., Morais Cabral, J., Pfuetzner, R.A., Kuo, A., Gulbis, J.M., Cohen, S.L., Chait, B.T., and MacKinnon, R. (1998). The structure of the potassium channel: molecular basis of K⁺ conduction and selectivity. *Science (New York, N.Y)* *280*, 69-77.

Fields, H.L. (1987). *Pain* (New York: McGraw-Hill Book Co.).

Fry, M., Maue, R.A., and Moody-Corbett, F. (2004). Properties of *Xenopus* Kv1.10 channels expressed in HEK293 cells. *J Neurobiol* *60*, 227-235.

Gunthorpe, M.J., Harries, M.H., Prinjha, R.K., Davis, J.B., and Randall, A. (2000). Voltage- and time-dependent properties of the recombinant rat vanilloid receptor (rVR1). *The Journal of physiology* *525 Pt 3*, 747-759.

Herrera, L., Hinrichs, M.V., Frias, J., Gutkind, S., and Olate, J. (1997). Dual transduction signaling by a *Xenopus* muscarinic receptor: adenylyl cyclase inhibition and MAP kinase activation. *J Cell Biochem* *65*, 75-82.

Hinman, A., Chuang, H.H., Bautista, D.M., and Julius, D. (2006). TRP channel activation by reversible covalent modification. *Proceedings of the National Academy of Sciences of the United States of America* 103, 19564-19568.

Hirsch, N., Zimmerman, L.B., and Grainger, R.M. (2002). *Xenopus*, the next generation: *X. tropicalis* genetics and genomics. *Dev Dyn* 225, 422-433.

Hoshi, T., Zagotta, W.N., and Aldrich, R.W. (1991). Two types of inactivation in Shaker K⁺ channels: effects of alterations in the carboxy-terminal region. *Neuron* 7, 547-556.

Hu, H.Z., Gu, Q., Wang, C., Colton, C.K., Tang, J., Kinoshita-Kawada, M., Lee, L.Y., Wood, J.D., and Zhu, M.X. (2004). 2-aminoethoxydiphenyl borate is a common activator of TRPV1, TRPV2, and TRPV3. *The Journal of biological chemistry* 279, 35741-35748.

Iiri, T., Herzmark, P., Nakamoto, J.M., van Dop, C., and Bourne, H.R. (1994). Rapid GDP release from Gs alpha in patients with gain and loss of endocrine function. *Nature* 371, 164-168.

Jancso, G., Kiraly, E., and Jancso-Gabor, A. (1977). Pharmacologically induced selective degeneration of chemosensitive primary sensory neurones. *Nature* 270, 741-743.

Jerman, J.C., Brough, S.J., Prinjha, R., Harries, M.H., Davis, J.B., and Smart, D. (2000). Characterization using FLIPR of rat vanilloid receptor (rVR1) pharmacology. *British journal of pharmacology* 130, 916-922.

Jones, D.T. (1999). Protein secondary structure prediction based on position-specific scoring matrices. *Journal of molecular biology* 292, 195-202.

Jordt, S.E., Bautista, D.M., Chuang, H.H., McKemy, D.D., Zygmunt, P.M., Hogestatt, E.D., Meng, I.D., and Julius, D. (2004). Mustard oils and cannabinoids excite sensory nerve fibres through the TRP channel ANKTM1. *Nature* 427, 260-265.

Jordt, S.E., and Julius, D. (2002). Molecular basis for species-specific sensitivity to "hot" chili peppers. *Cell* 108, 421-430.

Jordt, S.E., McKemy, D.D., and Julius, D. (2003). Lessons from peppers and peppermint: the molecular logic of thermosensation. *Current opinion in neurobiology* 13, 487-492.

Jordt, S.E., Tominaga, M., and Julius, D. (2000). Acid potentiation of the capsaicin receptor determined by a key extracellular site. *Proceedings of the National Academy of Sciences of the United States of America* 97, 8134-8139.

Julius, D. (2005). From peppers to peppermints: natural products as probes of the pain pathway. *Harvey lectures* 101, 89-115.

Julius, D., and Basbaum, A.I. (2001). Molecular mechanisms of nociception. *Nature* 413, 203-210.

Jung, J., Lee, S.Y., Hwang, S.W., Cho, H., Shin, J., Kang, Y.S., Kim, S., and Oh, U. (2002). Agonist recognition sites in the cytosolic tails of vanilloid receptor 1. *The Journal of biological chemistry* 277, 44448-44454.

Kandel, E.R., Schwartz, J.H., and Jessell, T.M. (2000). *Principles of neural science*, 4th edn (New York: McGraw-Hill, Health Professions Division).

Kim, H.J., Li, Q., Tjon-Kon-Sang, S., So, I., Kiselyov, K., and Muallem, S. (2007). Gain-of-function Mutation in TRPML3 Causes the Mouse Varitint-Waddler Phenotype. *The Journal of biological chemistry* 282, 36138-36142.

Kiss, L., and Korn, S.J. (1998). Modulation of C-type inactivation by K⁺ at the potassium channel selectivity filter. *Biophysical journal* 74, 1840-1849.

Kohda, K., Wang, Y., and Yuzaki, M. (2000). Mutation of a glutamate receptor motif reveals its role in gating and delta2 receptor channel properties. *Nature neuroscience* 3, 315-322.

Kwan, K.Y., Allchorne, A.J., Vollrath, M.A., Christensen, A.P., Zhang, D.S., Woolf, C.J., and Corey, D.P. (2006). TRPA1 contributes to cold, mechanical, and chemical nociception but is not essential for hair-cell transduction. *Neuron* 50, 277-289.

Latorre, R., Brauchi, S., Orta, G., Zaelzer, C., and Vargas, G. (2007). ThermoTRP channels as modular proteins with allosteric gating. *Cell calcium* 42, 427-438.

Lin, H., Zhang, H.F., Jiao, H.C., Zhao, T., Sui, S.J., Gu, X.H., Zhang, Z.Y., Buyse, J., and Decuypere, E. (2005). Thermoregulation responses of broiler chickens to humidity at different ambient temperatures. I. One week of age. *Poult Sci* 84, 1166-1172.

Lishko, P.V., Procko, E., Jin, X., Phelps, C.B., and Gaudet, R. (2007). The ankyrin repeats of TRPV1 bind multiple ligands and modulate channel sensitivity. *Neuron* 54, 905-918.

Liu, B., and Qin, F. (2005). Functional control of cold- and menthol-sensitive TRPM8 ion channels by phosphatidylinositol 4,5-bisphosphate. *J Neurosci* 25, 1674-1681.

Liu, J., and Siegelbaum, S.A. (2000). Change of pore helix conformational state upon opening of cyclic nucleotide-gated channels. *Neuron* 28, 899-909.

Liu, Y., Jurman, M.E., and Yellen, G. (1996). Dynamic rearrangement of the outer mouth of a K⁺ channel during gating. *Neuron* 16, 859-867.

Long, S.B., Campbell, E.B., and Mackinnon, R. (2005a). Crystal structure of a mammalian voltage-dependent Shaker family K⁺ channel. *Science (New York, N.Y)* 309, 897-903.

Long, S.B., Campbell, E.B., and Mackinnon, R. (2005b). Voltage sensor of Kv1.2: structural basis of electromechanical coupling. *Science (New York, N.Y)* 309, 903-908.

Lopez-Barneo, J., Hoshi, T., Heinemann, S.H., and Aldrich, R.W. (1993). Effects of external cations and mutations in the pore region on C-type inactivation of Shaker potassium channels. *Receptors & channels* 1, 61-71.

Loukin, S.H., Vaillant, B., Zhou, X.L., Spalding, E.P., Kung, C., and Saimi, Y. (1997). Random mutagenesis reveals a region important for gating of the yeast K⁺ channel Ykc1. *The EMBO journal* 16, 4817-4825.

Loumont, C. (1984). Current Distribution of the Genus *Xenopus* in Africa and Future-Prospects. *Revue Suisse de Zoologie* 91, 725-746.

Lukacs, V., Thyagarajan, B., Varnai, P., Balla, A., Balla, T., and Rohacs, T. (2007). Dual regulation of TRPV1 by phosphoinositides. *J Neurosci* 27, 7070-7080.

Macpherson, L.J., Dubin, A.E., Evans, M.J., Marr, F., Schultz, P.G., Cravatt, B.F., and Patapoutian, A. (2007). Noxious compounds activate TRPA1 ion channels through covalent modification of cysteines. *Nature* 445, 541-545.

Matta, J.A., and Ahern, G.P. (2007). Voltage is a partial activator of rat thermosensitive TRP channels. *The Journal of physiology* 585, 469-482.

McKemy, D.D., Neuhauser, W.M., and Julius, D. (2002). Identification of a cold receptor reveals a general role for TRP channels in thermosensation. *Nature* 416, 52-58.

Minor, D.L., Jr., Masseling, S.J., Jan, Y.N., and Jan, L.Y. (1999). Transmembrane structure of an inwardly rectifying potassium channel. *Cell* 96, 879-891.

Myers, B.R., and Julius, D. (2007). TRP channel structural biology: new roles for an old fold. *Neuron* 54, 847-850.

Navarro, B., Kennedy, M.E., Velimirovic, B., Bhat, D., Peterson, A.S., and Clapham, D.E. (1996). Nonselective and G betagamma-insensitive weaver K⁺ channels. *Science (New York, N.Y)* 272, 1950-1953.

Nilius, B. (2007). TRP channels in disease. *Biochimica et biophysica acta* 1772, 805-812.

Oh, U., Hwang, S.W., and Kim, D. (1996). Capsaicin activates a nonselective cation channel in cultured neonatal rat dorsal root ganglion neurons. *J Neurosci* 16, 1659-1667.

Ou, X., Blount, P., Hoffman, R.J., and Kung, C. (1998). One face of a transmembrane helix is crucial in mechanosensitive channel gating. *Proceedings of the National Academy of Sciences of the United States of America* 95, 11471-11475.

Peier, A.M., Moqrich, A., Hergarden, A.C., Reeve, A.J., Andersson, D.A., Story, G.M., Earley, T.J., Dragoni, I., McIntyre, P., Bevan, S., and Patapoutian, A. (2002a). A TRP channel that senses cold stimuli and menthol. *Cell* 108, 705-715.

Peier, A.M., Reeve, A.J., Andersson, D.A., Moqrich, A., Earley, T.J., Hergarden, A.C., Story, G.M., Colley, S., Hogenesch, J.B., McIntyre, P., *et al.* (2002b). A heat-sensitive TRP channel expressed in keratinocytes. *Science (New York, N.Y)* 296, 2046-2049.

Premkumar, L.S., Agarwal, S., and Steffen, D. (2002). Single-channel properties of native and cloned rat vanilloid receptors. *The Journal of physiology* 545, 107-117.

Prescott, E.D., and Julius, D. (2003). A modular PIP2 binding site as a determinant of capsaicin receptor sensitivity. *Science (New York, N.Y)* 300, 1284-1288.

Prober, D.A., Zimmerman, S., Myers, B.R., McDermott, B.M., Jr., Kim, S.H., Caron, S., Rihel, J., Solnica-Krezel, L., Julius, D., Hudspeth, A.J., and Schier, A.F. (2008). Zebrafish TRPA1 channels are required for chemosensation but not for thermosensation or mechanosensory hair cell function. *J Neurosci* 28, 10102-10110.

Rohacs, T., Lopes, C.M., Michailidis, I., and Logothetis, D.E. (2005). PI(4,5)P2 regulates the activation and desensitization of TRPM8 channels through the TRP domain. *Nature neuroscience* 8, 626-634.

Ryu, S., Liu, B., Yao, J., Fu, Q., and Qin, F. (2007). Uncoupling proton activation of vanilloid receptor TRPV1. *J Neurosci* 27, 12797-12807.

Sadja, R., Smadja, K., Alagem, N., and Reuveny, E. (2001). Coupling Gbetagamma-dependent activation to channel opening via pore elements in inwardly rectifying potassium channels. *Neuron* 29, 669-680.

Saito, S., and Shingai, R. (2006). Evolution of thermoTRP ion channel homologs in vertebrates. *Physiol Genomics* 27, 219-230.

Serrano, R., and Rodriguez-Navarro, A. (2001). Ion homeostasis during salt stress in plants. *Current opinion in cell biology* 13, 399-404.

Siemens, J., Zhou, S., Piskorowski, R., Nikai, T., Lumpkin, E.A., Basbaum, A.I., King, D., and Julius, D. (2006). Spider toxins activate the capsaicin receptor to produce inflammatory pain. *Nature* 444, 208-212.

Smith, G.D., Gunthorpe, M.J., Kelsell, R.E., Hayes, P.D., Reilly, P., Facer, P., Wright, J.E., Jerman, J.C., Walhin, J.P., Ooi, L., *et al.* (2002). TRPV3 is a temperature-sensitive vanilloid receptor-like protein. *Nature* 418, 186-190.

Su, Z., Zhou, X., Haynes, W.J., Loukin, S.H., Anishkin, A., Saimi, Y., and Kung, C. (2007). Yeast gain-of-function mutations reveal structure-function relationships conserved among different subfamilies of transient receptor potential channels. *Proceedings of the National Academy of Sciences of the United States of America* 104, 19607-19612.

Tombola, F., Pathak, M.M., and Isacoff, E.Y. (2006). How does voltage open an ion channel? *Annual review of cell and developmental biology* 22, 23-52.

Tominaga, M., Caterina, M.J., Malmberg, A.B., Rosen, T.A., Gilbert, H., Skinner, K., Raumann, B.E., Basbaum, A.I., and Julius, D. (1998). The cloned capsaicin receptor integrates multiple pain-producing stimuli. *Neuron* 21, 531-543.

Venkatachalam, K., and Montell, C. (2007). TRP channels. *Annual review of biochemistry* 76, 387-417.

Voets, T., Janssens, A., Droogmans, G., and Nilius, B. (2004). Outer pore architecture of a Ca²⁺-selective TRP channel. *The Journal of biological chemistry* 279, 15223-15230.

Voets, T., Prenen, J., Vriens, J., Watanabe, H., Janssens, A., Wissenbach, U., Boddling, M., Droogmans, G., and Nilius, B. (2002). Molecular determinants of permeation through the cation channel TRPV4. *The Journal of biological chemistry* 277, 33704-33710.

Winter, J. (1987). Characterization of capsaicin-sensitive neurones in adult rat dorsal root ganglion cultures. *Neuroscience letters* 80, 134-140.

Wood, J.N., Winter, J., James, I.F., Rang, H.P., Yeats, J., and Bevan, S. (1988). Capsaicin-induced ion fluxes in dorsal root ganglion cells in culture. *J Neurosci* 8, 3208-3220.

Xiao, R., Tian, J., Tang, J., and Zhu, M.X. (2007). The TRPV3 mutation associated with the hairless phenotype in rodents is constitutively active. *Cell calcium*.

Xu, H., Delling, M., Li, L., Dong, X., and Clapham, D.E. (2007). Activating mutation in a mucolipin transient receptor potential channel leads to melanocyte loss in varitint-waddler mice. *Proceedings of the National Academy of Sciences of the United States of America* 104, 18321-18326.

Xu, H., Ramsey, I.S., Kotecha, S.A., Moran, M.M., Chong, J.A., Lawson, D., Ge, P., Lilly, J., Silos-Santiago, I., Xie, Y., *et al.* (2002). TRPV3 is a calcium-permeable temperature-sensitive cation channel. *Nature* 418, 181-186.

Yeh, B.I., Kim, Y.K., Jabbar, W., and Huang, C.L. (2005). Conformational changes of pore helix coupled to gating of TRPV5 by protons. *The EMBO journal* 24, 3224-3234.

Yellen, G. (1998). The moving parts of voltage-gated ion channels. *Quarterly reviews of biophysics* 31, 239-295.

Yi, B.A., Lin, Y.F., Jan, Y.N., and Jan, L.Y. (2001). Yeast screen for constitutively active mutant G protein-activated potassium channels. *Neuron* 29, 657-667.

Yochim, J.M., and Spencer, F. (1976). Core temperature in the female rat: effect of ovariectomy and induction of pseudopregnancy. *Am J Physiol* 231, 361-365.

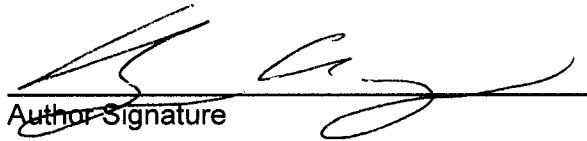
Zhou, X., Su, Z., Anishkin, A., Haynes, W.J., Friske, E.M., Loukin, S.H., Kung, C., and Saimi, Y. (2007). Yeast screens show aromatic residues at the end of the sixth helix anchor transient receptor potential channel gate. *Proceedings of the National Academy of Sciences of the United States of America* 104, 15555-15559.

Zhou, Y., Morais-Cabral, J.H., Kaufman, A., and MacKinnon, R. (2001). Chemistry of ion coordination and hydration revealed by a K⁺ channel-Fab complex at 2.0 Å resolution. *Nature* 414, 43-48.

PUBLISHING AGREEMENT

It is the policy of the University to encourage the distribution of all theses and dissertations. Copies of all UCSF theses and dissertations will be routed to the library via the Graduate Division. The library will make all theses and dissertations accessible to the public and will preserve these to the best of their abilities, in perpetuity.

I hereby grant permission to the Graduate Division of the University of California, San Francisco to release copies of my thesis or dissertation to the Campus Library to provide access and preservation, in whole or in part, in perpetuity.


Author Signature

12/30/08
Date